PHILOSOPHICAL TRANSACTIONS OF THE ROYAL SOCIETY A MATHEMATICAL, PHYSICAL & ENGINEERING SCIENCES

The Mechanical Properties of Pure Iron Tested in Compression over the Temperature Range 2 to 293 degrees K

T. L. Altshuler and J. W. Christian

Phil. Trans. R. Soc. Lond. A 1967 **261**, 253-287
doi: 10.1098/rsta.1967.0004

THE MECHANICAL PROPERTIES OF PURE IRON TESTED IN COMPRESSION OVER THE TEMPERATURE RANGE 2 TO 293 °K

By T. L. ALTSHULER and J. W. CHRISTIAN

Department of Metallurgy, University of Oxford

(*Communicated by W. Hume-Rothery, F.R.S.—Received* 28 *March* 1966—*Revised* 7 *September* 1966—*Read* 26 *January* 1967)

CONTENTS

The mechanical properties of pure iron single crystals and of polycrystalline specimens of a zone-refined iron have been measured in compression over the temperature and strain rate ranges 2·2 to 293 °K and 7×10^{-7} to 7×10^{-3} s^{-1} respectively. Various yield stress parameters were determined as functions of both temperature and strain rate, and the reversible changes in flow stress produced by isothermal changes of strain rate or by changes of temperature at constant strain rate were also measured as functions of temperature, strain and strain rate. Both the temperature variation of the flow stress and the strain rate sensitivity of the flow stress were generally identical for the single crystals (*ca.* 0·005/M carbon) and the polycrystalline specimens (*ca.* 9/M carbon). At low temperatures, the temperature dependence of the yield stress was smaller than that of the flow stress at high strains, probably because of the effects of mechanical twinning, but once again the behaviour of single and polycrystalline specimens was very similar. Below 10 °K, both the flow stress and the extrapolated yield stress were independent of temperature.

The results show that macroscopic yielding and flow at low temperatures are both governed by the same deformation mechanism, which is not very impurity sensitive, even in the very low carbon range covered by the experiments. The flow stress near 0 °K is *ca.* $5{\cdot}8 \times 10^{-3}\ \mu$ where μ is the

Vol 261. A. 1121. (Price 13*s.* 6*d*; U.S. $2.00) 32 [Published 8 June 1967

shear modulus. On the basis of a model for thermally activated flow, the activation volume at low temperatures (high stresses) is found to be *ca.* $5b^3$. The exponent in the empirical power law for the dislocation velocity against stress relation is *ca.* 3 near room temperature, but becomes quite large at low temperatures. The results indicate that macroscopic deformation at low temperatures is governed by some kind of lattice frictional stress (Peierls–Nabarro force) acting on dislocations.

1. Introduction

It is now generally accepted that the rapid increase of the macroscopic yield stress of a body-centred cubic metal with decreasing temperature is associated with the stress needed to move unpinned dislocations through appreciable distances. The relation between the temperature and strain rate sensitivities of the flow stress at finite strains indicates that the flow is thermally activated. The operative short-range process has been variously identified as a Peierls–Nabarro force (Basinski & Christian 1960; Conrad & Schoeck 1960; Conrad 1961, 1963; Christian & Masters 1964*a*, *b*), the cross slipping of screw dislocations (Brown & Ekvall 1962) or the interaction of dislocations with dispersed impurities (Stein, Low & Seybolt 1963).

In experiments on the grain size dependence of the yield stress in iron, Heslop & Petch (1956) showed that the contribution to the parameter σ_0 which arises from interstitial impurities is approximately independent of temperature. A similar result has been obtained in several investigations of the thermally activated flow at high strains, and this observed insensitivity of the temperature and strain rate sensitivities to impurity content has been the main experimental justification for rejecting the hypothesis that dislocation–impurity interactions are rate controlling at low temperatures. Recently, however, different results have been obtained at very low impurity levels. Johnston (1962) has shown that the temperature dependence of the flow stress previously measured in lithium fluoride crystals was largely due to impurities, and Lawley, Van den Sype & Maddin (1962–3) found a change in the shape of the flow stress against temperature curve after giving molybdenum crystals ten zone passes. Finally, Stein *et al.* (1963) prepared iron crystals of very low carbon content and reported that this reduced the difference in yield stress between room temperature and 77 °K to about one-half of the value usually found in less pure crystals.

The present paper describes the results of a comprehensive investigation into the deformation behaviour of pure iron in polycrystalline and single crystal form over the temperature range 2·2 to 293 °K. The tests were made in compression in order to avoid problems associated with necking or cleavage at low temperatures. A recently discovered complication in the interpretation of results from single crystals of b.c.c. metals is the unusually large orientation dependence of the yield stress which has been found at low temperatures (Rose, Ferriss & Wulff, 1962; Guiu & Pratt 1966; Stein & Low 1966; Stein 1967; Bowen, Christian & Taylor 1967). This orientation dependence has not been studied in the present work, but its existence must be kept in mind. In view of the importance of the results of Stein *et al.*, particular attention has been paid to the influence of small amounts of carbon on the properties measured. We were enabled to do this only because of Dr Stein's generous gift of three of his iron crystals.

PHILOSOPHICAL TRANSACTIONS OF THE ROYAL SOCIETY A MATHEMATICAL, PHYSICAL & ENGINEERING SCIENCES

2. Experimental

(a) *Materials and preparation of specimens*

Three single crystals of very pure iron prepared at General Electric Research Laboratories and presented to us by Dr Stein had the approximate compositions shown in table 1 (Stein 1963; Stein *et al.* 1963). Each crystal measured approximately $1{\cdot}25 \times 0{\cdot}100 \times 0{\cdot}075$ in. and was orientated so that the two side faces were $(1\bar{2}1)$ and *ca.* $(94\bar{1})$ while the long axis was *ca.* $[\bar{1}49]$. Individual specimens were prepared so that the compression axis coincided with this long axis: the orientations of the three crystals are shown in figure 1.

Table 1. Single crystal iron: impurities, parts per million by weight

impurity	crystals 1 and 2	crystal 3
C	0·005	40
N_2	< 3	< 3
O_2	~ 19	< 34
H_2	3	3
Mn	10	10
P	20	20
Si	60	60
Ni	400	400
Cr	100	100
Mo	100	100
Cu	100	100
Al	100	100
V	trace	trace

The above chemical composition was reported by Stein *et al.* (1963) and Stein (1963).

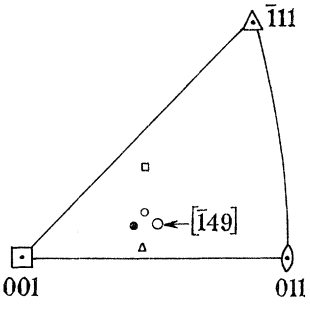

Figure 1. Orientations of iron single crystals. Crystals 1 and 2 contained *ca.* 0·005/M carbon; crystal 3 contained 40/M carbon. ○, Crystal no. 1; ●, specimen run 1–2β; △, crystal no. 2; □, crystal no. 3.

Rectangular compression test pieces were prepared from pieces of approximately 0·250 in. length cut from the crystals with a fine jewellers' saw. After coating with nail polish, a specimen was clamped in a specially constructed jig and the ends ground flat and parallel on 400 G followed by 600 G carborundum paper until the length was reduced to 0·187 in. Very great care was taken to minimize surface damage, and to ensure that the compression faces were accurately parallel and normal to the compression axis within 10^{-3} rad. After removal of the nail polish, the dimensions of the specimen were measured with a microscope, and it was weighed in order to determine more accurately the cross-sectional area. The specimens were tested without further annealing; the thickness of the deformed layer

at the specimen ends is estimated to have been less than 35 μm on the basis of work by Samuels (1956-7, 1957-8), and experiments were made to ensure that this did not affect the stress-strain behaviour appreciably (see below). Specimens were handled at all times with tweezers, the tips of which were coated with polyethylene.

Cylindrical specimens were prepared from parts of the as-received crystals by careful turning on a lathe with the use of cuts first of 0·001 in. and then of 0·0005 in., followed by light grinding with 600 G carborundum paper. Specimens were cut from the cylindrical crystal of 0·056 in. diameter and chemically polished in a freshly prepared solution of 5 g oxalic acid, 150 ml. water and 10 ml. of a 30 % solution of hydrogen peroxide (Stein *et al.* 1963). The specimen was permitted to roll continuously during polishing which was continued for 6 min, removing about 37 μm from the surface. Each specimen was then held in a special jig and the ends ground flat and parallel with 400 G and 600 G carborundum paper, after which it was given a final polish of three minutes in oxalic acid solution. The final specimen dimensions were: length 0·100 in. and diameter 0·050 in.

TABLE 2. POLYCRYSTALLINE IRON: IMPURITIES, PARTS PER MILLION BY WEIGHT

impurity		impurity	
C	10	Cu	7
O_2	11	Pb	< 1 (n.d.)
N_2	< 1	Mg	< 5
H_2	0·08	Mn	< 0·01
S	7	Mo	< 5 (n.d.)
Al	< 15	Ni	20
Sb	< 5 (n.d)*	P	9
As	< 5 (n.d.)	Si	10
Be	< 0·2	Sn	< 5 (n.d.)
B	< 5	Ti	< 1 (n.d.)
Cd	< 5 (n.d.)	W	< 5 (n.d.)
Ca	< 10 (n.d.)	V	< 1 (n.d.)
Cr	5	Zn	< 10 (n.d.)
Co	5	Zr	< 1 (n.d.)

* n.d. means not detected.

The above chemical composition was reported by Battelle Memorial Institute.

The specimens prepared in this way were clearly slightly deformed at the surface, and the possibility exists that not all the damage was removed by chemical polishing. To test this point, a rectangular specimen was deformed in compression at 77 °K to a stress of 28·4 Kg/mm^2 at 0·20 % plastic strain, and then unloaded. This specimen was machined into a standard cylindrical specimen and re-tested at 77 °K. The yield stress was then 28·2 Kg/mm^2, and the stress-strain curve appeared to be a continuation of that for the rectangular specimen. This test shows that any residual work hardening introduced into a cylindrical specimen during preparation was less than the equivalent of 0·1 % plastic compressive strain.

Polycrystalline specimens were made from a sample of zone refined iron prepared at the Battelle Memorial Institute, Columbus, Ohio with the analysed composition shown in table 2. The iron was cold-swaged without intermediate annealing to give rods of diameter *ca.* 0·070 in. Cylindrical compression test pieces were then prepared by the methods already described for single crystals, except that chemical polishing was not used. The specimens of length 0·100 in. and diameter 0·0505 in. were placed together in an alumina crucible and annealed for 1 h at 500 °C in a dynamic vacuum of $< 5 \times 10^{-7}$ torr. The temperature was

selected because there is some evidence that it provides maximum ductility at low temperatures. Several specimens were etched in the oxalic acid solution to reveal the grain boundaries. Over most of the cross section the grain size was quite uniform, and the mean grain diameter was *ca.* 0·013 mm. Larger grains near the outside had a mean diameter of *ca.* 0·04 mm. X ray examination showed an absence of any marked preferred orientation in the annealed specimens.

In preliminary investigations some compression specimens were prepared from a 0·050 in. diameter swaged rod without turning on a lathe and using a different jig for the grinding of the end faces. These specimens were annealed at 500 °C in a vacuum of 10^{-5} torr and were found to have a hardness of 99·6 d.p.n. in comparison with 78·5 d.p.n. for the specimens prepared later. Subsequent testing of the specimens gave results with appreciable scatter and this may be due both to improper removal of swaging defects and failure to grind the end faces accurately perpendicular to the cylindrical axis of the specimen. In appendix I it is shown that a very small angle between the axis and the normal to the end face results in appreciable error in a compression test.

The 'good' polycrystalline compression specimens are identified as Fe PX2 in the subsequent discussion; occasional reference may be made to the earlier specimens as Fe PX1. Single crystals are referred to as SX1, 2 or 3 for the three orientations shown in figure 1, and are followed by a specimen code number; thus SX2–3 is specimen 3 from crystal 2.

Three polycrystalline tensile specimens of total length 1 in. and gauge length 0·510 in. were also prepared from the Battelle iron. The diameter tapered very slightly from 0·0505 in. at the ends of the gauge length to 0·0503 in. at the centre. These specimens were intended to provide a check on the compression tests, and were annealed with the Fe PX2 compression specimens. Unfortunately the final grain size of the tensile specimen was much larger and was non-uniform, there being several large grains extending over the entire gauge length with smaller grains embedded in them.

(*b*) *Mechanical testing*

Compression and tensile tests were made on a Polanyi type machine fitted with a cryostat. The machine was similar to that described by Adams (1959), and the cryostat was adapted from the N.R.C. type (White 1962; Basinski 1959). The moving crosshead was screw driven from an electronically controlled motor with a switching arrangement enabling any one of five preset speeds to be selected at will. The fastest and slowest speeds differed by a factor of 50 and the time taken for a change between any two speeds was less than $\frac{1}{4}$ s. The cross head was driven through a gear box with a sliding shaft change and output to input speed ratios of 1:1, 0·1:1, and 0·01:1; for some of the tests a ratio of 10:1 was also available. The combination of motor speeds and gear ratios thus provided a very wide range of strain rates. The position of the crosshead was shown on a mechanical counter which indicated each 0·001 in. of travel, and a small voltage was also injected into the recorder to give visual blips at intervals of 0·001 in. The crosshead speeds were calibrated before each run.

The load was measured by a strain gauge dynamometer which was mounted on the moving crosshead, the $\frac{1}{4}$ in. diameter stainless steel tension rod being hung from the dynamometer via a universal joint. The stainless steel compression tube, concentric with the tension rod,

was $\frac{1}{2}$ in. outside diameter and $\frac{3}{8}$ in. inside diameter, and was rigidly attached to the supporting frame. The dynamometer measured a maximum load of 500 Lb., and was arranged to give a d.c. output to a Sunvic high speed recorder. The dynamometer and associated circuits were frequently calibrated over the whole range by dead weight loading, but day-to-day calibrations were obtained by means of a 'throw-off' switch which imposed a fixed fictitious load. This circuit used a resistor of very high stability and the relationship between the throw-off and the dead weight calibration did not change during the whole period of use. The normal sensitivity used was 2 kg/in., and 14 suppression steps were needed to cover the full load range. The zero suppression circuit used two accurate decade resistance boxes, and was carefully calibrated for linearity.

Tension tests were made with a jig using friction grips which were self-alining through universal joints. Two compression jigs were used. The first, of conventional design, had hardened high carbon steel anvils and could be used for specimens of any dimensions up to $\frac{3}{8}$ in. in diameter and $\frac{3}{4}$ in. in length. The loading arrangement utilized a sphere on the tension rod in contact with a hollow cone on the upper moving part of the compression jig. The second compression jig was a semi-automatic device which allowed up to twenty-one specimens of the fixed dimensions given above to be tested in sequence without disassembling the apparatus or changing the temperature. The specimens, preloaded into a feed-tube, were centred between the compression anvils in turn by an externally operated pawl mechanism. After the completion of a test, the specimen was ejected by the feed pawls into a chute, and a new specimen placed in position. In this machine, the anvils were made from martensitic stainless steel, and the top anvil was a sphere on which a flat surface had been ground and polished. This anvil protruded through a supporting ring arranged so that any very slight lack of parallelism in the end faces of the specimen could be corrected by the anvil. A more detailed description of the semi-automatic compression jig will be published elsewhere (see also Altshuler 1964); in the low temperature tests, it resulted in very great economy of time and of liquid hydrogen and helium.

The main disadvantage of the testing machine was the appreciable machine softness caused by the long stainless steel tension rod and compression tube. The softness is particularly troublesome in compression tests, because of small specimen dimensions, and is an undesirable feature when measuring incremental changes of stress due to changes of strain rate. It was not possible in the present work to measure directly the strain in the specimen, so the machine hardness was carefully measured for each compression jig and corrections were made to the apparent strains and strain rates.

(*c*) *Cryostat*

The specimen was sealed into a chamber which was filled with helium gas, and was in thermal contact with a second, upper chamber which could contain either a gas or a cryogenic fluid, admitted by an externally controlled needle valve. The upper chamber was used to maintain the specimen temperature above or below that of the liquid in the main Dewar by means of an electrical heater or by pumping after admitting liquid. These two chambers were surrounded by an isolating chamber which was either evacuated, or contained helium exchange gas. This chamber was immersed directly in the cryogenic fluid in the inner Dewar vessel, which was also provided with a vacuum seal, since low temperatures obtained

by reducing the vapour pressure above cryogenic fluids were more readily reached by pumping this vessel as well as the chamber immediately above the specimen.

The specimen temperature was determined either by measuring the vapour pressure of the cryogenic fluid or by using platinum and carbon resistance thermometers in ranges 60 to 273 and 0 to 77 °K respectively.

3. Preliminary experiments

(*a*) *Effects of lubricants: barrelling*

Various attempts were made to reduce the friction between specimen and compression anvils which leads to barrelling. Lubricants tried included molybdenum disulphide, powdered graphite and teflon; all were unsatisfactory, especially at low temperatures. The yield stress and stress-strain curves of a series of niobium specimens tested at room temperature with and without lubricants were all similar. It was concluded that the best conditions for obtaining uniform deformation and minimizing buckling were to use height: diameter ratios of 2:1 and to test without lubricants.

An incremental loading technique is sometimes suggested as an effective way of reducing barrelling. An experiment in which a specimen was alternately loaded and unloaded to give successive strain increments of 2% produced no difference in the stress–strain curve up to *ca.* 30% axial deformation.

In the present experiments, the shape of the stress-strain curve was not required accurately, but it was important to know whether barrelling introduced significant errors into the determination of the changes in axial stress $\Delta\sigma$ caused by changes of temperature or strain rate. In order to test this point, three Fe PX2 specimens were deformed to strains of 17 to 25% at temperatures of 13·95, 77 and 293 °K respectively, producing noticeable barrelling. The dimensions of the specimens were then measured under a microscope and the barrelling correction suggested by Read, Markus & McCaughey (1952) was applied. The ratio σ_0/σ_m where σ_0 is the axial stress of a uniformly deformed specimen at given strain and σ_m is the axial stress measured in a barrelled specimen, was found to be 0·952, 0·943 and 0·968 in the three specimens. The deviation of *ca.* 5% is considered acceptable since it can be shown that

$$\Delta\sigma_0/\sigma_0 = \Delta\sigma_m/\sigma_m,$$

where $\Delta\sigma_0$ is the required stress increment and $\Delta\sigma_m$ is the stress increment actually measured (see appendix II).

(*b*) *Comparison of tension and compression tests*

Figure 2 shows curves of axial stress against logarithmic strain for Fe PX2 specimens tested in tension and compression. The tension tests show consistently lower values of flow stress at given strain, but the general shapes of the curves are very similar in the two cases. The difference in stress is almost certainly due to the large and non-uniform grain size of the tensile specimens. The curves also illustrate the rapid decrease in strain to fracture in the tensile specimens as the temperature is lowered, and this is the main reason for choosing to test in compression at low temperatures.

It can be seen from figure 2 that the temperature dependence of the yield and flow stress is approximately the same in both tension and compression. Measurements of the strain

rate sensitivity in tension and compression have also been made at 293, 77 and 20·4 °K and in each case the stress increment for a given change of strain rate was essentially independent of the mode of deformation.

Finally, a series of tests were carried out on polycrystalline niobium specimens in tension and compression. The grain sizes are believed to have been more comparable here, and in any case grain size variation is less significant, since the factor k_y of the Petch equation is nearly zero for niobium. These tests showed that the curve of yield stress against temperature in compression agreed very closely with the curve previously determined in tension

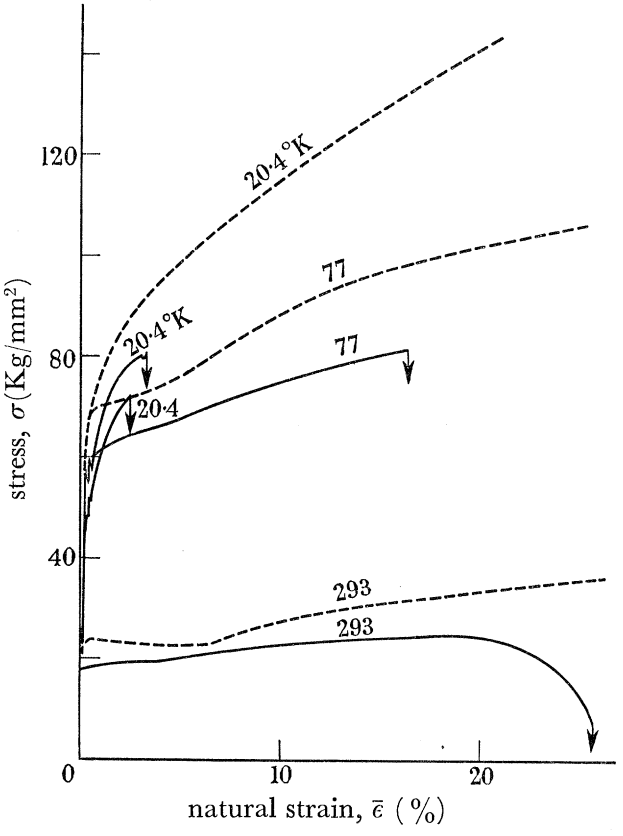

FIGURE 2. Curves of axial stress against strain for polycrystalline specimens PX2 tested in tension (——) and compression (– – –). Strain rate, $\dot{\epsilon}$, $\approx 5 \times 10^{-4}$ s^{-1}.

for material of the same purity (Christian & Masters 1964). In a series of tests at 20 °K, the yield stress in compression was found consistently to equal the fracture stress in tension.

As a result of these tests, and of the measurements of barrelling errors, it is concluded that there are no essential differences in the temperature and strain rate sensitivities of the flow stress when measured in tension and compression. As might be expected, shear stress against shear strain curves for single crystals tested in tension and compression do sometimes show appreciable differences in the extents and slopes of stages I and II (Bowen *et al.* 1967) but these are not relevant to the present investigation.

4. General deformation behaviour

(a) *Polycrystalline specimens*

The annealed polycrystalline specimens after etching in Gorsuch's reagent (Gorsuch 1959) to reveal dislocations had an etch-pit density of *ca.* 4×10^7 cm^{-2} in favourably orientated grains. Figure 3 shows typical curves of stress against strain for these specimens at a fixed plastic strain rate of 4×10^{-4} s^{-1} and various temperatures from 2·19 to 293 °K. The discontinuous yield point disappears between 90 and 77 °K at this strain rate, but evidence of inhomogeneous (Luders band) deformation can be seen down to *ca.* 60 °K. The yielding behaviour is dependent on the strain rate, and the yield point reappears at 20 °K when the strain rate is reduced to 4×10^{-6} s^{-1}.

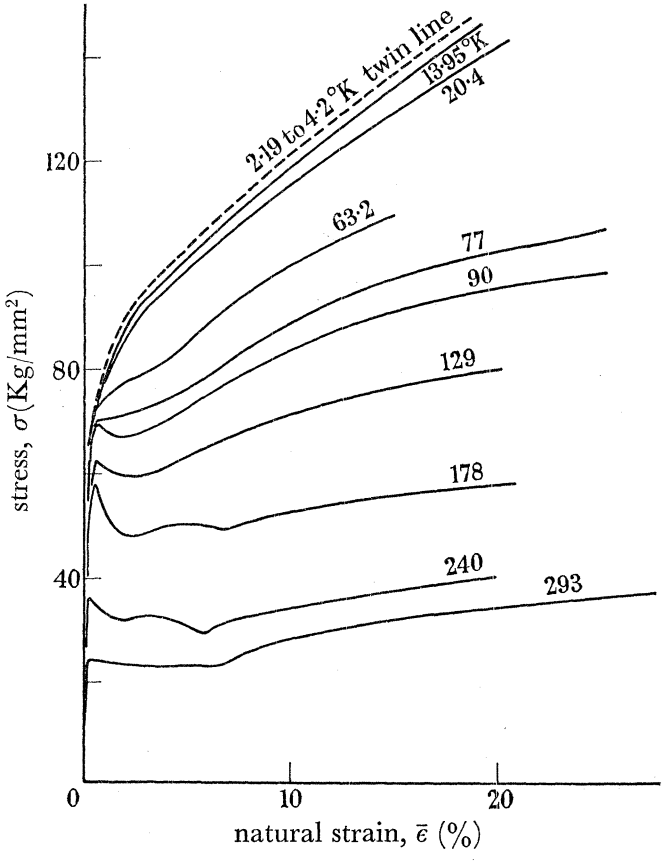

FIGURE 3. Curves of axial stress against strain for polycrystalline iron tested in compression at $\dot{\epsilon} = 5 \times 10^{-4}$ s^{-1}.

At a strain rate of 4×10^{-4} s^{-1} slight load drops due to twinning appear at about 90 °K during the transition from elastic to plastic deformation. At lower temperatures, these load drops become more frequent, and occur at variable stresses during the elastic loading; at 11 °K considerable twinning was observed even after yielding. Below 10 °K, deformation was entirely by twinning, and the curve given for 2·19 °K represents the successive peak stresses attained after each load drop.

The curves of load against extension on the recorder chart were found to be very linear over appreciable ranges of strain after the initial inhomogeneous deformation. Because

of difficulties connected with the transition from discontinuous to smooth yielding and with early twinning at low temperatures, none of the usual methods of measuring a yield stress or a proof stress could be considered to be very accurate. An arbitrary parameter, the extrapolated yield stress, has therefore been defined by extrapolating backwards the initial linear part of the curve of load against extension curve to meet the elastic line, as shown in figure 4. Although similar extrapolation techniques have been widely used, usually in connexion with plots of true stress against strain, it is emphasized here that the extrapolated yield stress ($\sigma_{ex.}$) is *not* to be identified with the friction stress term (σ_i) of the Hall–Petch equation (see, for example, Phillips & Chapman 1965). In this paper, $\sigma_{ex.}$ is regarded as a convenient experimental parameter which is dependent on the flow stress and work hardening rate after the onset of uniform deformation at *ca.* 8 % strain. Its relation, if any, to yield-

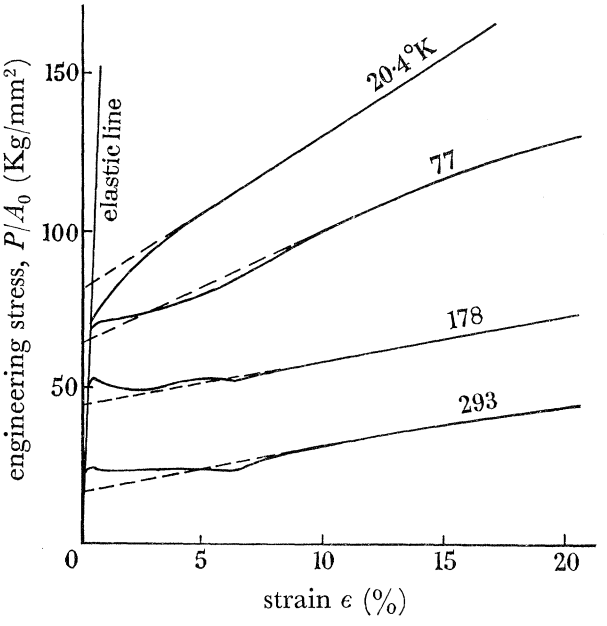

FIGURE 4. To illustrate the procedure used to obtain the arbitrary parameter, σ_{ex}, at various temperatures. $\dot{\epsilon} \approx 5 \times 10^{-4}$ s^{-1}.

ing has to be established by comparison with the measured behaviour of the lower yield stress over the temperature and strain rate range for which this latter quantity is well defined.

Metallographic examination of specimens deformed at room temperature revealed the usual wavy slip lines; at low temperatures slip lines were very difficult to detect under the optical microscope, but twins were clearly visible, and the amount of twinning correlated reasonably well with the total strain magnitude of load drops on the stress against strain curves. Etch pit determination of dislocation densities in the strained specimens was not attempted, as the dislocation density at quite low strains became too high to resolve individual pits.

(*b*) *Single crystals*

The initial dislocation density of the single crystals, as measured by etch-pitting the (112) face, was *ca.* 5×10^6 cm^{-2}. In this work, no detailed study has been made of work hardening behaviour, and shear stress against shear strain curves have not been computed

because of the difficulties caused by twinning at low temperatures. Compression tests on single crystals are therefore plotted as curves of stress against axial (logarithmic) strain; the stress is the resolved shear stress in the initial orientation but no allowance is made for change of orientation during deformation. Most crystals were not deformed to more than *ca.* 20% strain; assuming single slip to be operative throughout this deformation, the true shear stress at 20% axial strain would be *ca.* 0·9 of the plotted value, and the shear strain would be *ca.* 37%.

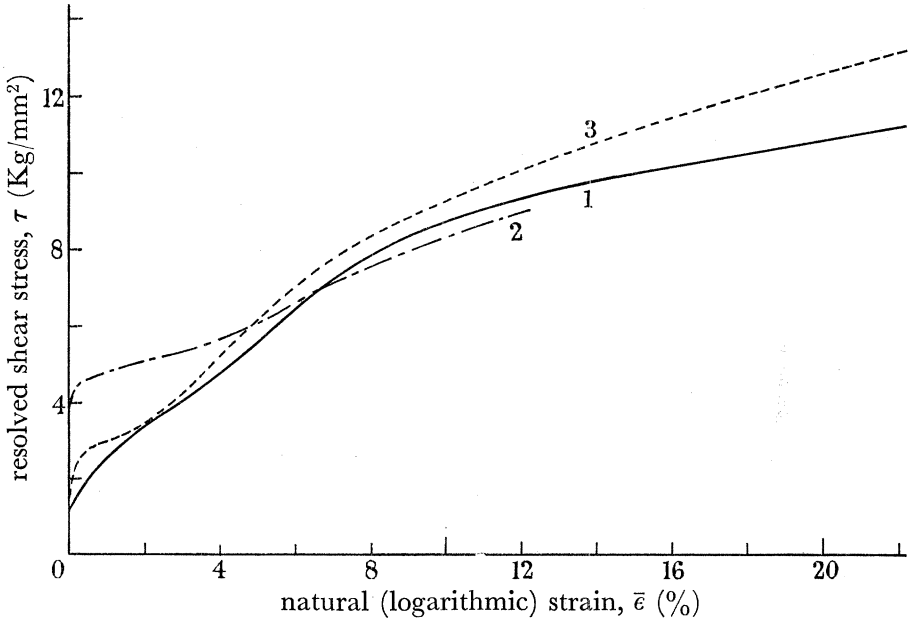

FIGURE 5. Curves of shear stress against axial strain for single crystals of iron tested in compression at 293 °K. The stress is not corrected for axis rotation during deformation. Curve 1, Fe SX1 (0·005/M C); test 1–1; $\dot{\epsilon} = 3 \times 10^{-4}$ s^{-1}; 2, Fe SX1 (0·005/M C); test 1–7; $\dot{\epsilon} = 6 \times 10^{-4}$ s^{-1}; 3, Fe SX3 (44/M C); test 3–5, $\dot{\epsilon} = 3 \times 10^{-4}$ s^{-1}.

Figure 5 shows stress against strain curves for three single crystals deformed at 293 °K. Two of the crystals were of identical orientation and purity and the high yield stress in test 1–7 is believed to be a result of plastic deformation occurring during improper preparation of the cylindrical specimen. This particular machining technique involved holding the specimen in a four-jaw chuck and in a lathe collet, and was used only for four specimens; later specimens were held in a brass tube with araldite.

The yield stress of the crystal containing 44/M carbon (test 3–5) is somewhat higher than that found in test 1–1 for the very pure iron, and there seems to be a slight Luders region, or rather a region of lower work hardening. In both curves a tendency towards three stage hardening can be seen, as already noted for iron by Keh (1965). More pronounced three stage hardening is found in niobium (Mitchell, Foxall & Hirsch 1963; Taylor & Christian 1965) and tantalum (Mitchell & Spitzig 1965). The tendency for stage I to diminish as the purity of the material increases can be seen in figure 5, and is also found in niobium.

As previously reported (Altshuler & Christian 1966), crystals of rectangular cross section generally yielded with a large load drop attributed to twinning at 77 °K, the twinning stress being little dependent on purity. Figure 6 shows a group of tests at 77 °K on circular

specimens all prepared from crystal 1, compared with one test (1–3) on a rectangular specimen. It is apparent that the yield stresses are all nearly equal; the slightly higher curve 1–8 was obtained from one of the four specimens believed to have been deformed slightly during preparation (see above). The rather high yield stresses shown in this figure, and the corre-

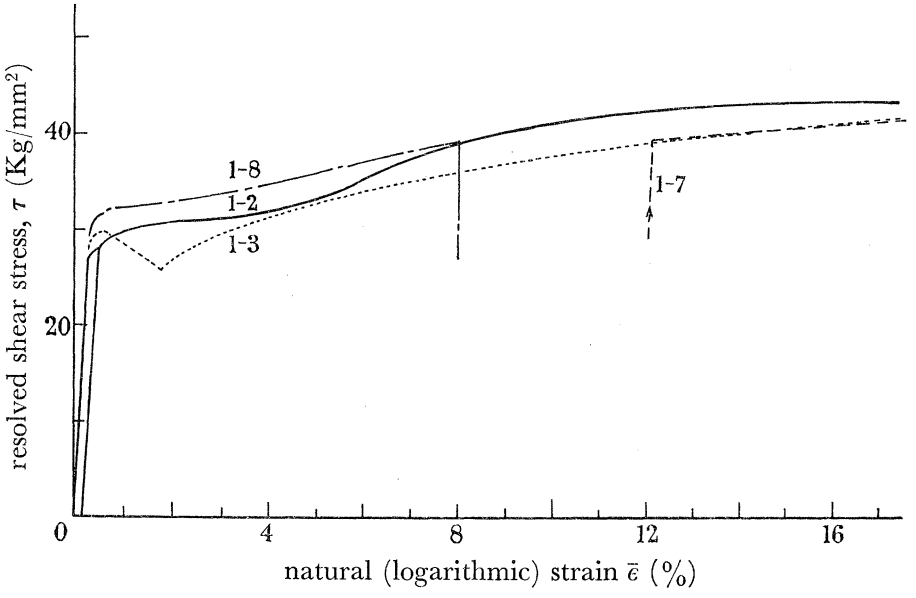

FIGURE 6. Curves of shear stress against axial strain for single crystals of iron tested in compression at 77 °K. The stress is not corrected for axis rotation during deformation. $\dot{\epsilon} = 6 \times 10^{-4}$ s^{-1}.

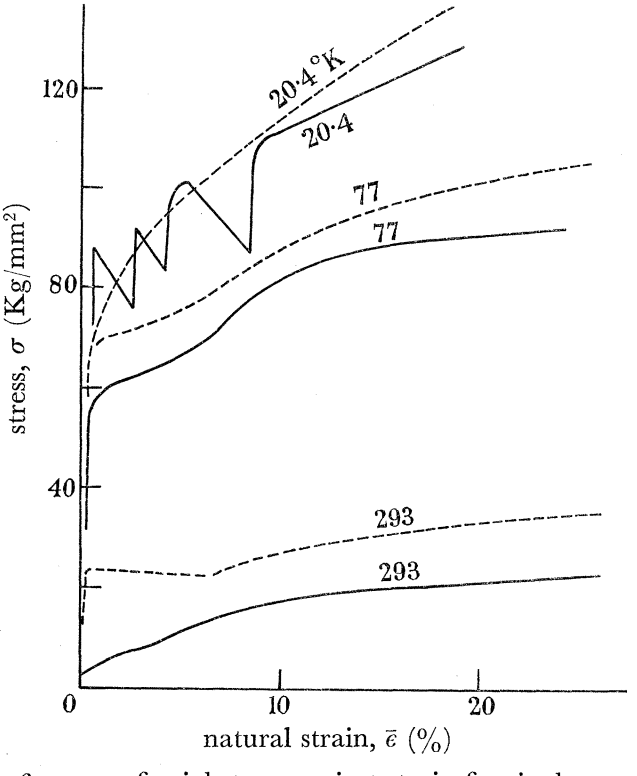

FIGURE 7. Comparison of curves of axial stress against strain for single crystals (——) and polycrystalline specimens (– – –) of iron tested in compression at three different temperatures. $\dot{\epsilon} \approx 5 \times 10^{-4}$ s^{-1}.

sponding twinning stresses for rectangular specimens, contrast with the low yield value reported by Stein *et al.* at 77 °K.

Stress-strain curves for single crystals at 20 °K have been published previously (Altshuler & Christian 1966) and show uniform slip deformation after an initial period of twinning. Figure 7 gives a comparison between the axial stress against strain behaviour of the very pure single crystal 1 and the slightly impure polycrystals over the temperature range 20 to 293 °K. Clearly the purer material does not have a lower temperature sensitivity of the yield stress than the less pure polycrystalline material over the range 77 to 293 °K, and over the total range 20 to 293 °K the purer material actually has a rather greater temperature dependence.

5. Yielding phenomena

(*a*) *Shape of curves of load against extension*

At room temperature, discontinuous yielding behaviour in polycrystalline specimens was quite variable, as illustrated in the recorder charts for three different tests reproduced in figure 8. The first test shows a single load drop followed by a Luders region, the second test shows double load drops whilst in the third test only the second load drop is apparent. At 180 °K all tests were of the second type, and two tests were interrupted after the first and second load drops respectively in order to make measurements of diameter along the

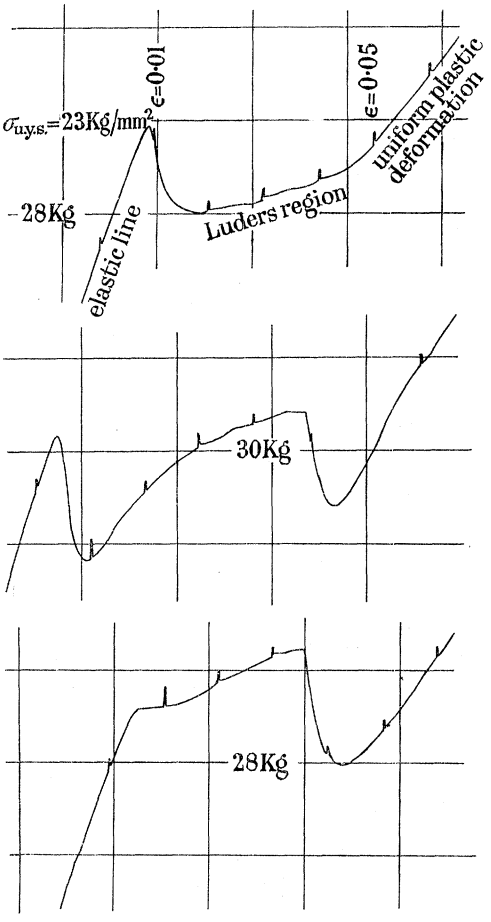

Figure 8. Tracings from recorder chart records of load drops during yielding in three different compression tests at 293 °K. $\dot{\epsilon} \approx 8 \times 10^{-4}$ s^{-1}.

length of the specimen. These results are shown in figure 9. In test 95, after the first yield drop, deformation is confined to *ca.* one-half of the specimen, through which a Luders band has apparently moved rapidly. After the second yield drop, test 98, the whole specimen has been deformed, although not uniformly. Apparently the first Luders front moved through only one-half of the specimen, which then continued to deform until another Luders front moved through the remainder and caused the second load drop.

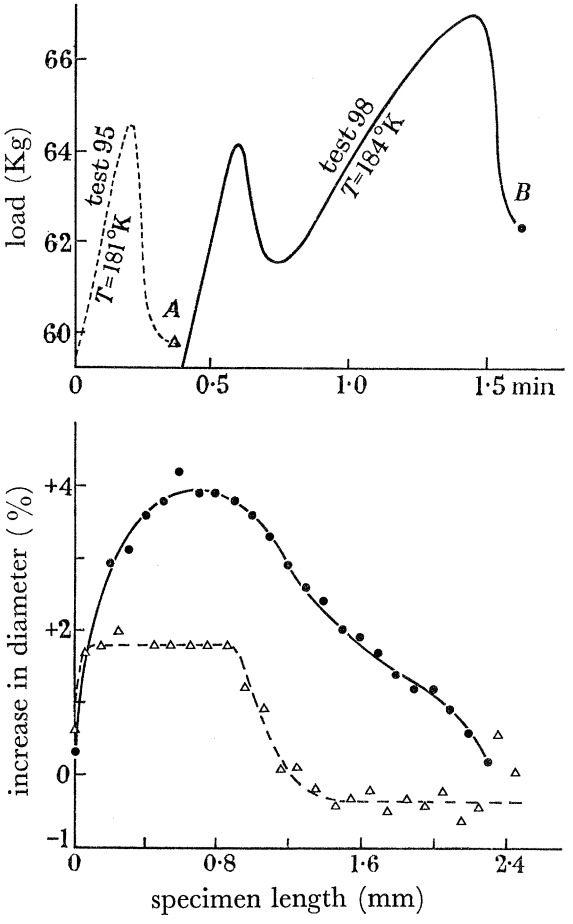

FIGURE 9. Curves of load against extension (taken directly from the chart records) for two different tests at *ca.* 180 °K are shown in the upper figure, and the lower figure gives the measured changes in specimen diameter for these two tests.

(*b*) *Temperature and strain rate variation of upper and lower yield stresses*

Figure 10 shows plots of upper yield stress against strain rate at four different temperatures. Within the rather wide scatter of the results, the u.y.s. is a linear function of the logarithm of the strain rate at each of these temperatures, and the slope of the line does not change appreciably with temperature. Figure 11 shows a similar plot of the lower yield stress at 293 °K. The data indicate a linear relation between l.y.s. and logarithm of strain rate. The dashed lines show the 95% probability limits of the true regression line for an infinite number of tests, and the larger limiting bar indicates the expected scatter limits for 95% of the data. Similar regression plots with statistical analysis of data were made at other temperatures down to 90 °K. Although the slope of the plot at 273 °K is larger than at 293 °K, there is once again little variation of this slope with temperature over the whole range covered.

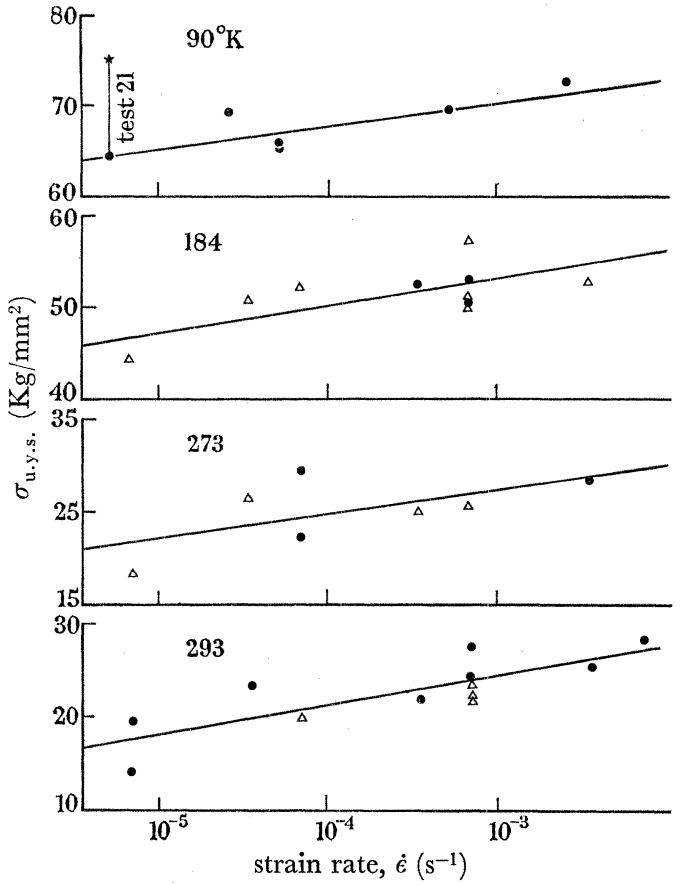

FIGURE 10. Plots of the upper yield stress against strain rate for polycrystalline iron tested in compression at various temperatures. ●, Tests giving single lower yield points; △, tests giving double lower yield points.

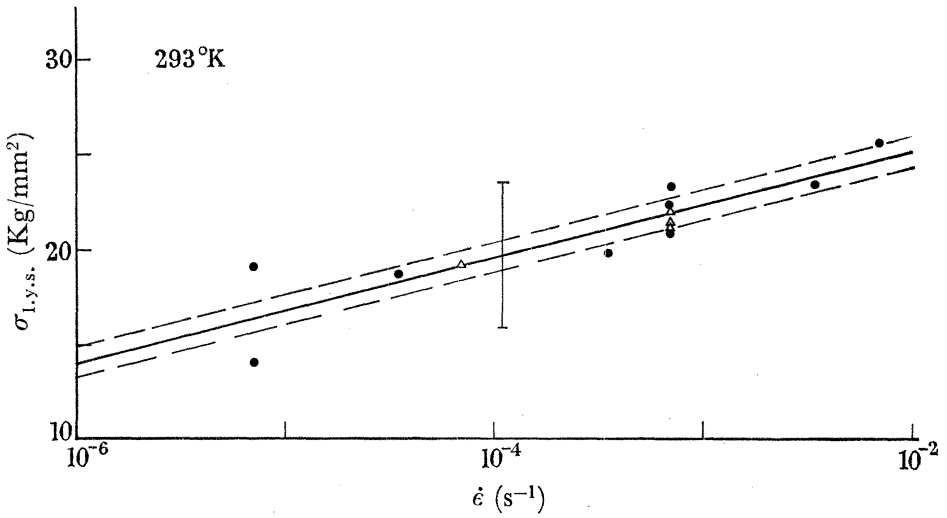

FIGURE 11. Plot of the lower yield stress against strain rate for polycrystalline iron tested in compression at 293 °K. Symbols as in figure 10. Dashed lines show the 95 % probability limits of the regression line, and the bar shows the expected scatter range for 95 % of the data.

Figure 12 gives the temperature variation of u.y.s. and l.y.s. for various strain rates. The curves are drawn for strain rates of $4 \times 10^{-4}\,s^{-1}$ and are obtained from the regression curves. Upper and lower yield stresses could be distinguished down to 90 °K at this strain rate, to 77 °K at $2{\cdot}25 \times 10^{-5}\,s^{-1}$, and to 20 °K at $4 \times 10^{-6}\,s^{-1}$.

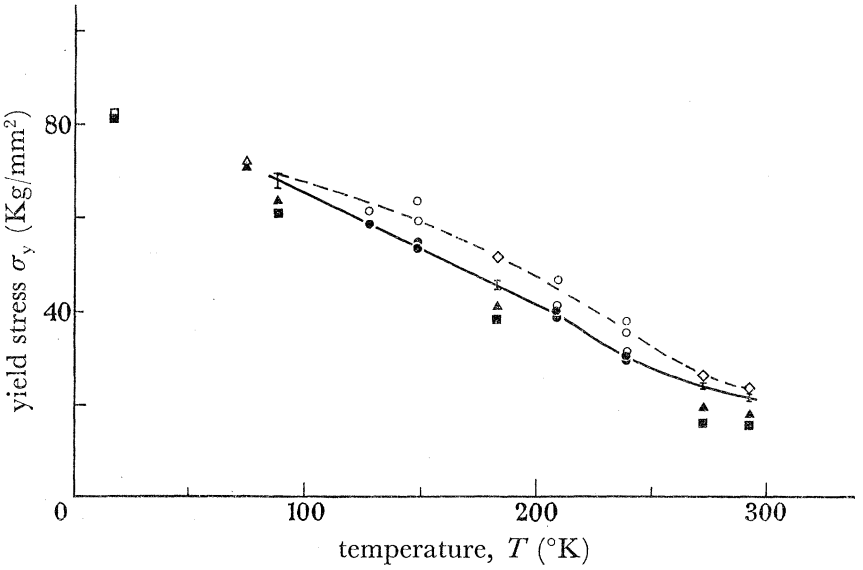

FIGURE 12. Temperature variation of upper and lower yield stresses of polycrystalline iron tested in compression at various strain rates. ◇, u.y.s. obtained from u.y.s.-$\dot{\epsilon}$ curves, $\dot{\epsilon} = 4 \times 10^{-4}$; ○, u.y.s. data, $\dot{\epsilon} \approx 5 \times 10^{-4}$; △, u.y.s. data, $\dot{\epsilon} = 2{\cdot}25 \times 10^{-5}$; □, u.y.s. data, $\dot{\epsilon} = 4 \times 10^{-6}$; I, l.y.s., 95 % probability of mean, $\dot{\epsilon} = 4 \times 10^{-4}$; ●, l.y.s. data, $\dot{\epsilon} \approx 5 \times 10^{-4}$; ▲, l.y.s. data, $\dot{\epsilon} = 2{\cdot}25 \times 10^{-5}$; ■, l.y.s. data, $\dot{\epsilon} = 4 \times 10^{-6}$; – – –, u.y.s. curve, $\dot{\epsilon} = 4 \times 10^{-4}$; ——, l.y.s. curve, $\dot{\epsilon} = 4 \times 10^{-4}$.

(*c*) *Extrapolated yield stresses*

Figure 13 shows the variation with temperature of extrapolated yield stress, defined in figure 4, for a constant strain rate of $5 \times 10^{-4}\,s^{-1}$. The limiting bars in this figure were determined from regression plots of $\sigma_{ex.}$ against $\log_{10} \dot{\epsilon}$, which was found to be a linear relation at each temperature as for the upper and lower yield stresses. An interesting feature of figure 13 is the apparent levelling of the curve below *ca.* 11 °K; the statistical analysis indicates that this is a real effect.

Several tests with the very pure single crystals are also plotted in figure 13. In these cases, the yield stresses plotted were obtained by extrapolation from *ca.* 2 % strain. Except at 293 °K, the points lie close to the polycrystalline curve.

The slopes of the regression lines of extrapolated yield stress against logarithm of strain rate varied more with temperature than did those of u.y.s. and l.y.s. The change in extrapolated yield stress for a tenfold change in strain rate has rather wide confidence limits, but there is a clear indication of a minimum strain rate sensitivity near 77 °K, with maxima at higher and lower temperatures. The behaviour contrasts with the smooth curve for the strain rate sensitivity of the flow stress obtained at constant strain and strain rate, which is plotted on the same figure (see figure 17 below). The minimum strain rate sensitivity near 77 °K corresponds to the disappearance of the upper and lower yield points at that temperature, and indicates that measurements of extrapolated yield stress in the presence and absence of a load drop on yielding are not comparable with one another.

At 4·2 °K it was not possible to obtain smooth plastic curves even after predeformation. However, the stresses at which three specimens twinned at 4·2 °K after differing strains at 13·95 °K were measured and were found to lie on the work-hardening curve obtained from the successive peak loads measured in direct deformation at 4·2 °K. These points were therefore extrapolated to the elastic line to give a parameter equivalent to the extrapolated yield stress at 4·2 °K.

A comparison of the temperature dependences of the extrapolated yield stresses of the two different sets of polycrystalline samples shows the temperature dependences to be identical, but the improperly prepared Fe PX 1 samples have consistently higher yield values with a greater scatter.

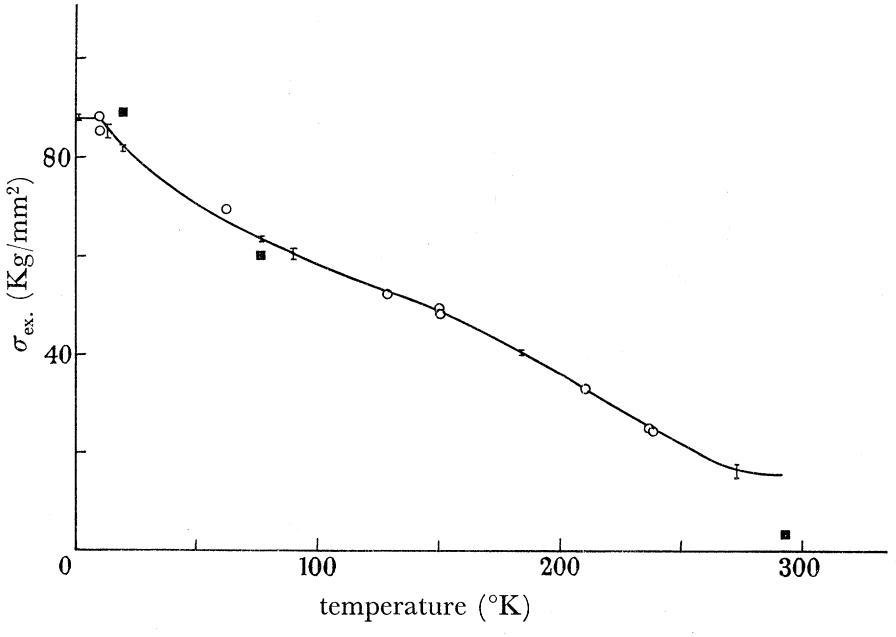

FIGURE 13. Temperature variation of the extrapolated yield stress of polycrystalline iron (○ = Fe PX 2) tested in compression. $\dot{\epsilon} = 5 \times 10^{-4}$ s^{-1}. Some single crystal yield stresses are plotted for comparison (■ = Fe SX 1). 95 % of the data are expected to be within the scatter band I.

6. FLOW STRESS MEASUREMENTS

(*a*) *Temperature dependence*

The temperature dependence of the flow stress at finite strains was measured by the usual thermal cycling procedure. Figure 14 shows a series of changes between 77 and 20·4 °K. Slight work softening was sometimes obtained on increasing the temperature (see the last change in figure 14), so all measurements were taken from the downward changes of temperature. The transition from elastic to plastic deformation after such a decrease of temperature was usually slightly rounded, and the stress increment was measured by extrapolating the plastic part of the curve at the lower temperature back to the elastic line. Load drops were not observed in any of these experiments, but at low temperatures there was sometimes a very slight initial period of low work hardening after a temperature change, so that the stress immediately following the change was higher than that obtained by extrapolating

the curve from higher strains. The error caused by uncertainty about whether the extrapolation procedure should or should not be used in such cases was very small.

The dependence of the flow stress difference between any two temperatures on stress or strain during work hardening was found to be small. Between 293 and 273 °K no dependence could be measured, between 90 and 60 °K there was possibly a very small increase in flow stress difference with strain, and between 77 and 20 °K there was a measurable increase in flow stress difference of about 30% over the whole strain range. Finally, no systematic variation with strain of flow stress difference between 20 and 13·95 °K was detectable. In some tests between these latter two temperatures, twins were formed at 13·95 °K with an accompanying load drop, but the measured difference in stress was the

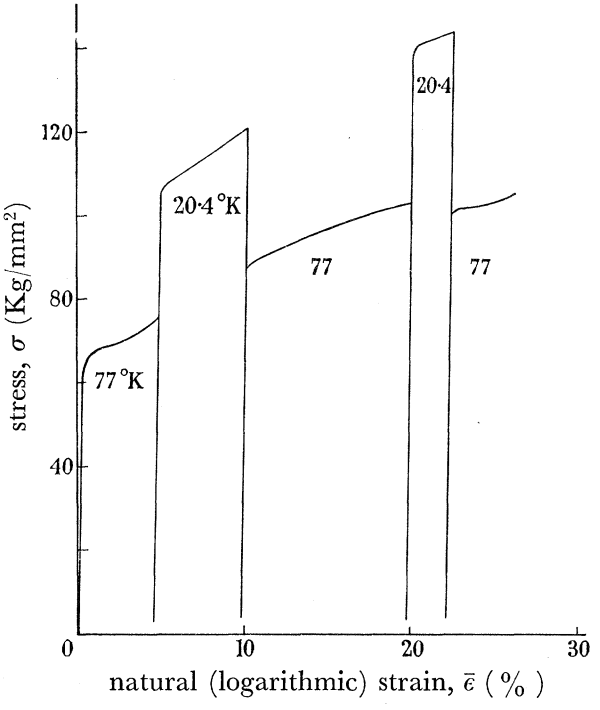

FIGURE 14. Thermal cycling test for polycrystalline iron tested in compression at 77 and 20·4 °K. $\dot{\epsilon} \approx 5 \times 10^{-4}\ s^{-1}$.

same as that found when a smooth curve was obtained at 13·95 °K. The transition from 13·95 to 4·2 °K always resulted in twin-induced load drops at the lower temperature, but the result just cited suggests that the measured stress increment gives the true flow stress increment for this temperature (Altshuler & Christian 1966).

Experiments were also made to test whether the change in stress between two temperatures depends upon the basic strain rate. A measurable effect was found only between 293 and 273 °K where the difference in flow stress is a linear function of the logarithm of the strain rate. This result has not previously been reported, but is related to the dependence of the strain rate sensitivity of iron on the basic strain rate near room temperature which was found by Basinski & Christian (1960) and Mordike & Haasen (1962), and is also reported later in this paper (figure 16).

Figure 15 gives the temperature dependence of the flow stress at a strain of 0·10 and a strain rate of $4 \times 10^{-4}\ s^{-1}$. The flow stress increases rapidly with decreasing temperature

down to *ca.* 11 °K, after which it becomes constant. A statistical analysis of the available data suggests that this is a real effect, as in the extrapolated yield stress curve (figure 13).

Figure 15 includes points from both the polycrystalline PX 2 samples and the pure single crystals. It is a remarkable result that all these points lie on one smooth curve, indicating to a high degree of accuracy that the temperature dependence of the flow stress does not depend on carbon content in the range of purities covered by these samples.

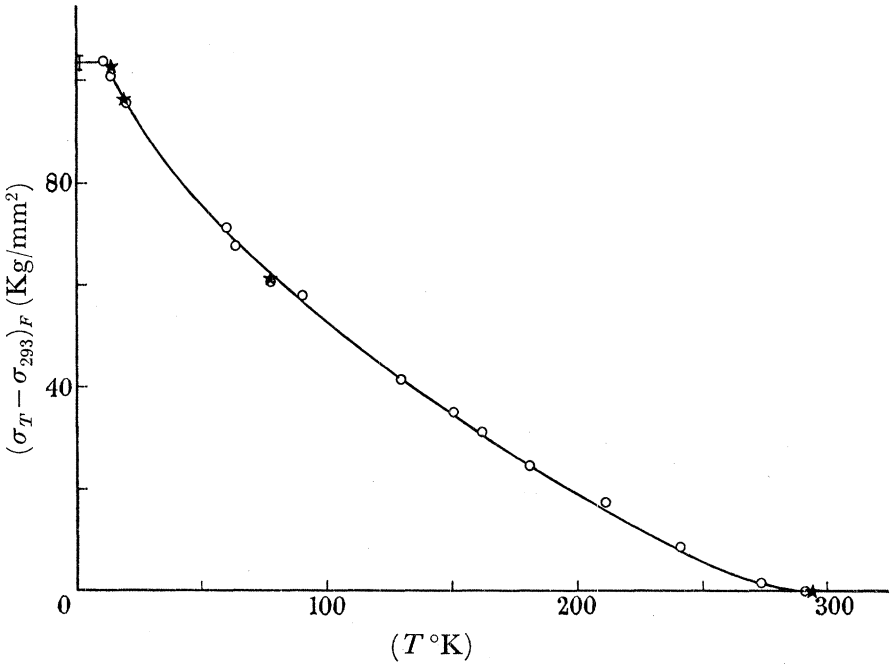

FIGURE 15. The temperature dependence of the flow stress for single crystals (★) and polycrystalline specimens (○) of iron tested in compression. $\dot{\epsilon} = 4 \times 10^{-4} s^{-1}$. The data points are taken at a strain of 10 %.

(*b*) *Strain rate dependence*

The procedure used in most measurements of strain rate sensitivity was to cycle one specimen between two different strain rates throughout the stress strain curve. The initial deformation was at the higher strain rate, and only *ca.* 10 % of the total strain was produced at the lower strain rate. It is therefore believed that the dislocation structure in these experiments was essentially that characteristic of the higher strain rate. Some tests were made with more complex programmes of changes in strain rate.

Changes of stress were always measured from upward changes of strain rate. Since strain rates were usually changed by the selector switch, rather than by means of a gearbox, the crosshead speeds were measured in each experiment. The measurements showed that the actual changes differed very little from those intended. In a few early tests at 20 °K between nominal strain rates of 4×10^{-4} and $4 \times 10^{-5} s^{-1}$, the crosshead speeds were not measured directly, but there is a 95 % probability that the error in the strain rate sensitivity is less than 5·3 % when calculated from the nominal speeds.

Tests were made at 293, 77 and 20 °K to verify that the strain rate sensitivity measured for tensile specimens was comparable to that measured for compression specimens. The results at 20 °K were inconclusive, since the tensile specimen fractured on making the second upward change of strain rate, but at the other two temperatures the tensile and

compression specimens gave the same values of strain rate sensitivity, despite the large difference in grain size and yield stresses already noted.

Plots of $(\Delta\sigma/\Delta \log_{10} \dot{\epsilon})_T$ against stress or strain show no systematic variation at any temperature except 20 °K, where there is an apparently linear increase of strain rate sensitivity with stress which extrapolates backwards to pass close to the origin. At all temperatures, single crystals had essentially the same strain rate sensitivities as the polycrystalline specimens, in agreement with the identical temperature dependence of flow stress for single and polycrystalline specimens. At 293 °K it was found that single crystals containing 44/M carbon had a slightly smaller strain rate sensitivity than those containing 0·005 /M carbon.

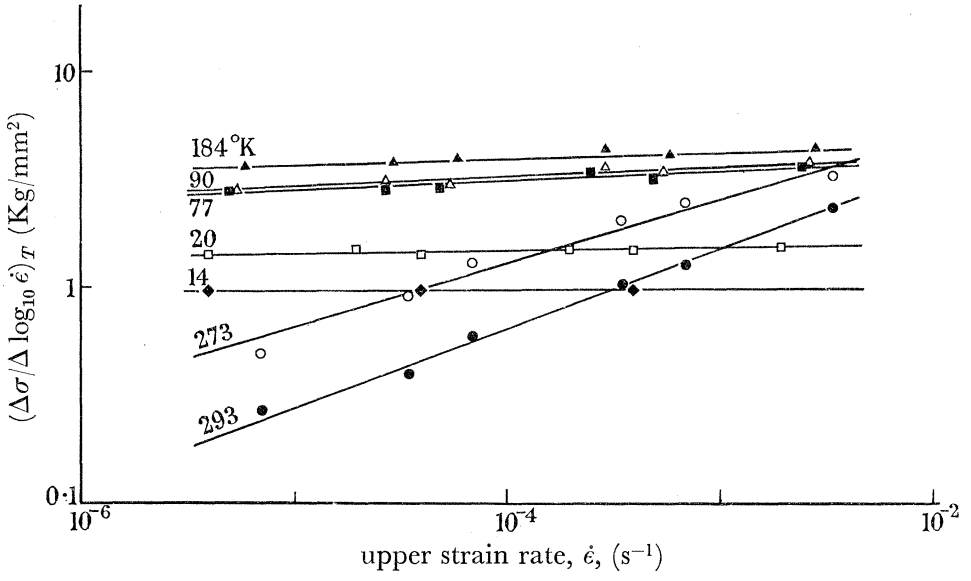

FIGURE 16. The strain rate sensitivity of polycrystalline iron as a function of the basic strain rate at various constant temperatures. The data points are taken at $\epsilon = 10\,\%$.

Measurements were also made of the variation of strain rate sensitivity with basic strain rate over a wide range of strain rates. Figure 16 gives this variation at a constant strain of 0·10, the plotted points being the average values of the data obtained from individual tests. At each temperature, the logarithm of the strain rate sensitivity may be represented as a linear function of the logarithm of the strain rate, but the variation is scarcely measurable at 184 °K and lower temperatures. Basinski & Christian (1960) found the strain rate sensitivity to be a linear function of the logarithm of the strain rate at 273 °K, but these results covered a much smaller range of strain rates.

The plots of strain rate sensitivity against temperature for various basic strain rates are given in figure 17. As reported by Basinski & Christian, the strain rate sensitivity has a broad maximum in the region of 180 °K. The present results show for the first time that the details of this curve depend on the basic strain rate, but the general form of the curve is similar for all the strain rates investigated. As already emphasized, figures 16 and 17 apply to both the polycrystalline and single crystal specimens.

Stein (1966) has recently reported measurements of the strain rate sensitivity of iron single crystals of widely varying carbon content tested in tension at 298 and 198 °K. At the higher temperature, he finds a smaller strain rate sensitivity for the crystals of higher

carbon content, in agreement with the present results. Stein also reports the strain rate sensitivity to be nearly independent of purity at 198 °K, and his reported values of strain rate sensitivity (after correcting a misprint) agree with those found in the present work.

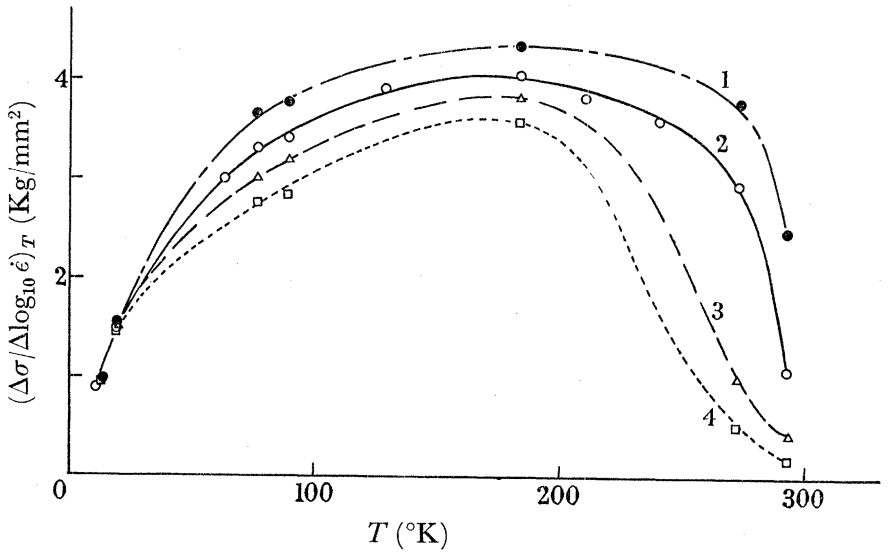

FIGURE 17. The strain rate sensitivity of polycrystalline iron as a function of temperature for various constant strain rates. The data points are taken at $\epsilon = 10\,\%$. Curve 1, $\dot{\epsilon} = 4 \times 10^{-3}$; 2, $\dot{\epsilon} = 4 \times 10^{-4}$; 3, $\dot{\epsilon} = 4 \times 10^{-5}$; 4, $\dot{\epsilon} = 4 \times 10^{-6}$.

7. COMPARISON OF YIELD AND FLOW STRESS RESULTS

(*a*) *Temperature dependence*

It was emphasized above that the extrapolated yield stress, $\sigma_{ex.}$ is an arbitrary parameter related to the flow stress and work hardening rate at finite strains. Previous attempts to use an extrapolation technique to obtain the parameter σ_i of the Hall–Petch equation derive from Cottrell (1958) and have been used by several workers. Mogford & Hull (1963), for example, found that values of σ_i and k_y of iron determined by extrapolation agreed within 3 % with the values determined by the grain size analysis at 293, 233 and 195 °K. However, Dingley (1963) found the extrapolated stress for iron decreased with increasing grain size, and Phillips & Chapman re-analysed Mogford & Hull's results and found differences of *ca.* 10 %. Lindley & Smallman (1963) reported good agreement between σ_i values for vanadium but no agreement for niobium, and Johnson (1962) found a large discrepancy for molybdenum. The error in an attempted theoretical justification of the procedure by Rosenfield (1962-3) was pointed out by Phillips & Chapman (1965).

Figure 18 shows a comparison of the temperature dependences of the lower yield stress, the extrapolated yield stress and the flow stress at a strain of 0·10, as determined in the present work. There is a close correlation between the extrapolated yield stress curve and the lower yield stress curve over the temperature range for which the latter was defined at a strain rate of $4 \times 10^{-4}\,s^{-1}$, and at a strain rate of $4 \times 10^{-6}\,s^{-1}$ this correlation extends down to 20 °K. Thus although the extrapolated yield stress is not to be identified with the friction stress on free dislocations, its temperature dependence does seem accurately to reflect that of the lower yield stress.

The temperature dependence of the yield stress is also equal to that of the flow stress over the temperature range 300 to 150 °K, confirming earlier results by Basinski & Christian (1960) and Conrad & Schoeck (1960). A surprising feature of figure 18, however, is that at low temperatures the yield stress increased less rapidly than the flow stress, which would not be expected if the temperature dependence of the yield stress arises entirely from the stress needed to maintain uniform dislocation velocity. Recent theories of yielding (Cottrell 1963) imply that the yield stress has a temperature dependence equal to or greater than that of the flow stress.

The change in slope of the yield stress curve for iron has been noted previously, although in earlier work the break seems to occur at lower temperatures in the region of 77 °K (Conrad 1960; Low 1963). Louat (1956) modified the original theory of dislocation unlocking to explain the break, but Erickson & Low (1957) showed that the change of slope was probably attributable to the onset of yielding by twinning. Their description requires

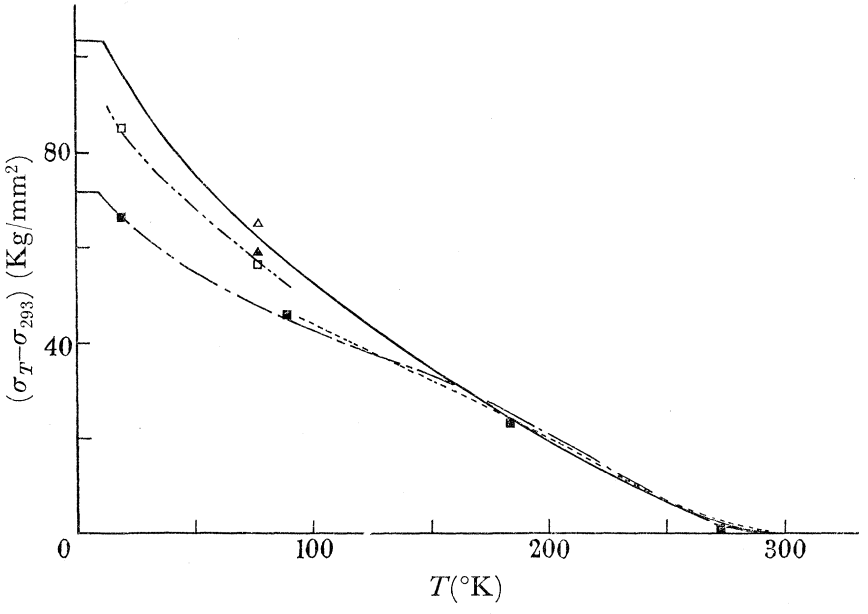

FIGURE 18. The temperature dependence of the yield and flow stresses of pure iron. △, Flow stress, $\bar{\epsilon} = 0{\cdot}10$ (Davidenkov & Chuman 1960); ▲, extrapolated flow stress, $\bar{\epsilon} = 0$ (Davidenkov & Chuman 1960); □, extrapolated yield stress, Fe SX1, $\dot{\epsilon} = 4 \times 10^{-4}$ s^{-1}; ■, lower yield stress, Fe PX2, $\dot{\epsilon} \approx 4 \times 10^{-6}$ s^{-1}; ——, flow stress Fe PX2 and FeSX1, $\bar{\epsilon} \approx 0{\cdot}10$, $\dot{\epsilon} = 4 \times 10^{-4}$ s^{-1}; —··—, extrapolated flow stress, Fe PX2, $\bar{\epsilon} = 0$, $\dot{\epsilon} = 4 \times 10^{-4}$ s^{-1}; — - —, extrapolated yield stress, Fe PX2, $\dot{\epsilon} = 4 \times 10^{-4}$ s^{-1}; – – – –, lower yield stress, Fe PX2, $\dot{\epsilon} = 4 \times 10^{-4}$ s^{-1}.

that deformation by twinning at low temperatures can take place at stresses smaller than those required for general yield, and it is suggested that the suppression ofdiscontinuous yielding below 77 °K is attributable to yield initiation by twinning.

Erickson and Low's description apparently conflicts with recent results which indicate that twin nucleation in silicon–iron (Hamer & Hull 1964) and pure iron (Altshuler & Christian 1966) is preceded by yielding. However, a lowering of the yield stress would be possible in polycrystalline materials if twins are nucleated in regions of high stress concentration and then are able to grow under applied stresses which are insufficient for general yielding. This description would also explain the results at low temperatures in figure 7,

where the twin stresses in single crystals are higher than the polycrystalline yield stresses, presumably because stress concentrations have been avoided.

It follows that the temperature dependence of the single crystal yield stress should be similar to that of the polycrystalline flow stress extrapolated to zero strain, rather than to that of the polycrystalline yield stress. Unfortunately there were insufficient data points to allow this flow stress curve to be determined accurately above 77 °K, but it is plotted in the region from 20 to 77 °K in figure 18 and shown to be in excellent agreement with the single crystal yield stress curve. Also, Davidenkov & Chuman (1960), using a quite different iron, obtain values for the flow stress difference between 239 and 77 °K at several different strains. The values at a strain of 0·10 plotted on figure 18 agrees with the flow stress curve for this strain determined in the present work, and the value extrapolated to zero strain agrees well with that obtained in the present work for the single crystal yield stress.

The remaining difficulty is to explain why the break in the polycrystalline yield curve occurs at 150 °K in the present results, instead of 77 °K as previously reported. Sleeswyk & Helle (1963) have found that the number of twinned grains in deformed polycrystalline iron increases gradually from $2\frac{1}{2}$ to 80% over the temperature range 157 to 77 °C, but it is difficult to believe that yielding is initiated by twinning in this region (Louat 1959; Erickson & Low 1959). However, it may be possible for a microtwin formed in a region of stress concentration to produce a larger plastic zone capable of initiating yielding. The extent of such a zone would depend on the size of the twin and the ratio of the applied stress to the friction stress (cf. Bilby, Cottrell & Swinden 1963, for the analogous case of a crack), and in the intermediate temperature region before twinning becomes general, the twin is merely acting as a more efficient dislocation source. However, in view of the present evidence that yielding stresses vary unexpectedly in single crystals of different orientations, there may well be some other explanation for the divergency of yield and flow stresses.

Comparison of the present results for the temperature dependences of yield and flow stresses with those previously published shows generally good agreement for comparable polycrystalline materials (see, for example, Arsenault 1964) although there are some minor discrepancies. Much of the published data, including the recent tensile work of Kossowksy & Brown (1966) on very similar material, shows a rather smaller change of stress in the range 200 to 300 °K. The reason for this is not known, but several mechanisms may be rate-controlling at high temperatures, and the flow may be impurity sensitive.

The agreement is much worse for single crystal results. The present yield stress curve agrees reasonably well with that of Edmondson (1961), but the temperature dependence is greater than that of Allen, Hopkins & McLennan (1956). The discrepancy between the two earlier sets of results is difficult to understand, since they were obtained in the same laboratory using crystals grown (by slightly different techniques) from the same material. A similar difficulty exists in regard to the present results and those of Stein *et al.* (1963) and Stein & Low, (1966), all of which were obtained with crystals prepared by Stein.

Stein *et al.* define the yield by the proportional limit and the 0·2% proof stress, and this accounts for part of the discrepancy since it is established (Conrad 1963) that the proportional limit often has a smaller temperature dependence than other measures of the yield

and flow. However, the twinning stresses in tension found by Stein & Low (1966) at 77 and 20 °K are also appreciably smaller than the present compression values, and these differences are not readily explained. It seems improbable that inadvertent pre-straining of the compression specimens could be causing high twin stress values, since such prestraining tends to suppress twinning, and little deviation from the elastic line was observed at temperatures below 77 °K. Moreover, the required increase in stress is much too large to be attributable to any probable amount of work hardening.

The present results are exceptional in that twins do not form until the applied stress reaches the value for macroscopic flow. In contrast, tests on purified niobium single crystals (Boucher 1966; Taylor, unpublished work) show the twinning stress at very low temperatures to be nearly temperature independent and below the extrapolated flow stress. Since it is now believed that twins are nucleated by slip, the different behaviour can be rationalised in terms of the availability of twin nuclei and/or stress concentrations (Altshuler & Christian 1966).

No comparable data exist with which to compare the observation that both the extrapolated yield stress and the flow stress of polycrystalline iron become temperature independent below *ca.* 10 °K. If this is a real effect, it may be connected with quantum-mechanical tunnelling through the barrier. Mott (1956) has discussed this possibility in connexion with experiments on low temperature creep (Glen 1956), and calculated that creep should be independent of temperature for cadmium below *ca.* 10 °K.

(*b*) *Strain rate dependence*

The upper yield stress, lower yield stress and extrapolated yield stress are all linear functions of the logarithm of the strain rate within the accuracy of the experiments, so that the strain rate sensitivity $(\Delta\sigma/\Delta \ln \dot{\epsilon})_T$ is independent of strain rate $\dot{\epsilon}$. Lean (1960) found the strain rate sensitivity of the lower yield stress to be constant with both temperature and strain rate (except at 293 °K) and his values agree well with the present results. However, the upper yield stress results of Petch (1964) in conjunction with dynamic data obtained by Campbell & Maiden (1958) and Marsh & Campbell (1963) are more complex. Petch finds that the strain rate sensitivity of the upper yield stress is constant at 77 °K, but varies linearly with the logarithm of the strain rate at 194 and 291 °K. The difference in the two sets of results is well outside the experimental error, but may be due to differences in purity. In the present work, for example, upper and lower yield stresses at 77 °K were only found at very low strain rates.

At most temperatures where comparison is possible, the magnitudes of the strain rate sensitivities of yield and flow stresses are similar. The strain rate sensitivities of the yield stresses are not so temperature dependent as that of the flow stress, and the well defined maximum in the latter at 180 °K is not apparent. The extrapolated yield stress has a low rate sensitivity at 77 °K, but this is probably related to the transition to yielding by twinning at normal strain rates. At high strains, deformation is believed to be effected mainly by dislocation motion, so that the flow stress remains sensitive to rate. The upper yield stress appears to be less rate sensitive than the flow stress at all temperatures except 293 °K.

The values of the strain rate sensitivity of the flow stress in the region 77 to 293 °K are in good agreement with the earlier results of Basinski & Christian (1960) and Conrad &

Frederick (1962). At low temperatures, the strain rate sensitivity is nearly independent of strain rate, but there is an appreciable variation with strain rate near room temperature in accordance with earlier results. This is discussed in § 9, but the question now arises why the same variation is not found for yield stresses. Simple models of yielding imply that the stress is determined by the mean dislocation velocity, so that the rate sensitivities of yield and flow stresses should behave in the same way. The results of Petch show the expected behaviour of the upper yield stress at room temperature, but introduce another discrepancy, since they indicate an equally large effect at 194 °K where the rate sensitivity of the flow stress is nearly constant. A major source of uncertainty in making all these comparisons arises from the difficulty in defining the true strain rate during yielding when the flow is localized and the dislocation density is changing rapidly. It is for this reason that conclusions regarding the mechanism of flow are best based on flow stress experiments at high strains.

(*c*) *Impurity sensitivity*

A main purpose of the investigation was further to examine the claim that impurities are responsible for a major part of the temperature sensitivities of yield and flow stresses. The evidence obtained is all negative. Although the yield stresses do not agree with those found by Stein & Low (1966), it is clear that both sets of results imply that much of the temperature sensitivity remains in carbon-free ion. Yield stresses are difficult to interpret, especially since the change with orientation is not understood, but it is especially noteworthy that the temperature and strain rate sensitivities of the flow stress for both types of iron were found to be identical over most of the temperature range. These results seem to substantiate previous conclusions that impurities contribute a stress term which is not very temperature dependent.

The experimental result is in agreement with theoretical arguments, such as those given by Christian & Masters (1964). Using a (shear) flow stress of 52 Kg/mm^2 at 0 °K, $b = 2{\cdot}48$ Å and assuming an interaction energy of 0·5 eV, the product of the distance between pinning points l and the 'activation distance' d is about 65 Å^2. Thus if $d = b$, the dislocation behaves as a rigid line, and *ca.* 10 at. % of pinning points would be required. Alternatively if the dislocation bends between nearest neighbour pinning points in the slip plane, d would have the improbably low value of 0·15 Å for an impurity content of 30 /M, and the flow stress at 0 °K would be 0·5 Kg/mm^2 when this content is reduced to 0·005/M. No changes in assumptions or reasonable variations in parameters seem able to overcome this difficulty; at the known impurity levels, the high flow stresses found at low temperatures cannot be attributed to dislocation-impurity interactions without adopting an impossibly high value for the interaction energy.

8. Rate theory of flow

The shapes of the curves of strain rate sensitivity against temperature (figure 17) are similar to those previously published (Christian & Masters 1964), but the present work shows for the first time the slight shift in the curve as the basic strain rate is changed. The results leave little doubt that the flow is thermally activated, and the usual assumption of a simple rate equation

$$G = H - TS = kT \ln (\nu/\dot{\epsilon}) \qquad (1)$$

enables the relevant parameters to be determined. In equation (1) G, H, S are respectively the free energy, enthalpy and entropy of activation, $\dot{\epsilon}$ is the axial strain rate, and the frequency factor ν is given by

$$\nu = \rho p b \phi \nu_0 = NAb\phi\nu_0, \tag{2}$$

where $\phi \approx \frac{1}{2}$, ν_0 is an atomic vibration frequency, b is the Burgers vector, ρ is the dislocation density, p is the average distance moved by a dislocation after an activation, N is the density of activation sites and A is the area of slip plane swept after an activation.

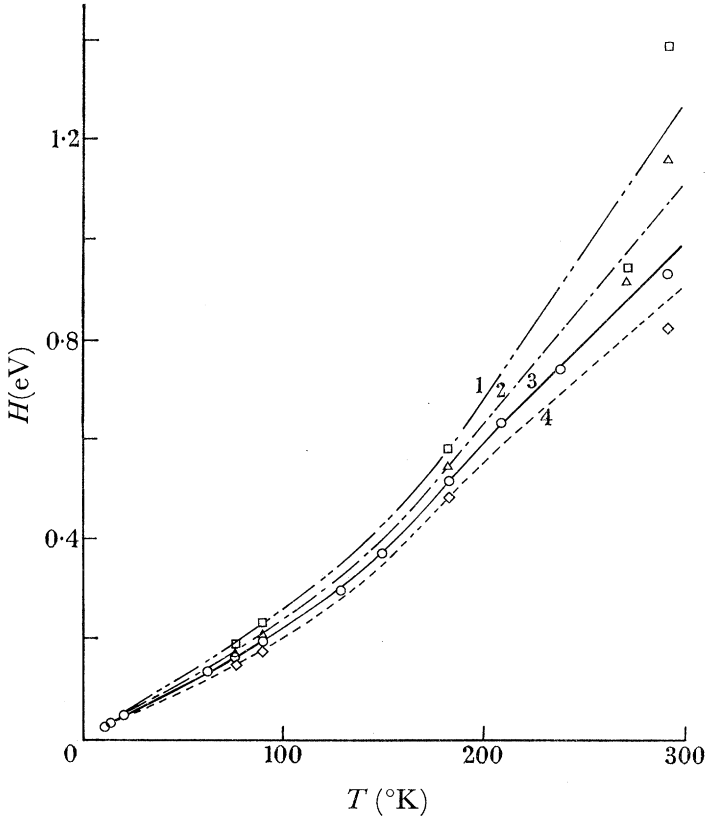

FIGURE 19. The activation enthalpy against temperature curve for various constant strain rates. Curve 1, $\dot{\epsilon} = 4 \times 10^{-6}$; 2, $\dot{\epsilon} = 4 \times 10^{-5}$; 3, $\dot{\epsilon} = 4 \times 10^{-4}$; 4, $\dot{\epsilon} = 4 \times 10^{-3}$; $\bar{\epsilon} = 0{\cdot}10$.

Shoeck (1965) has recently given a treatment of the rate theory which, although not free from assumptions, seems more satisfactory than earlier formulations. According to this theory, the activation enthalpy, H, and the activation volume, $v = -(\partial G/\partial \tau)$, are given without approximations by equations (6) and (10) of Christian & Masters (1964*b*). Figure 19 shows the variation of activation enthalpy with temperature determined in this way at various constant strain rates. As in previous work, H is nearly a linear function of temperature, but in contrast to the results of Masters and Christian, H/T in figure 19 actually *increases* slightly with temperature.

If the entropy of activation can be ignored, experimental determinations of H/kT give values of $\ln(\nu/\dot{\epsilon})$. Basinski & Christian (1960) found $H/kT \approx 27$ for iron over the temperature range 77–273 °K at a strain rate of $10^{-4}\,s^{-1}$; corresponding results in the present work are shown in figure 20. With a strain rate of $4 \times 10^{-4}\,s^{-1}$, H/kT seems to have a nearly constant value of 25 from 0 to 100 °K, and then to increase to *ca.* 37 at 300 °K. As discussed by

Christian & Masters (1964*b*) it is rather difficult to explain the higher values of ln ($v/\dot{\epsilon}$) unless the activation distance, p, is appreciably larger than b. It is not clear whether the variation with temperature of H/kT indicates a corresponding variation of v, or arises from the entropy term in equation (1).

The rate theory analysis requires that the density of moving dislocations does not change appreciably during a change of strain rate or temperature. Reasons for believing this assumption to be valid have been given previously (Christian 1964); the present results provide experimental evidence of a new kind. It follows from equations (1) and (2) that if v (and hence ρ) is not strain rate sensitive, each curve in figure 20 should be separated from its neighbours by $\Delta \ln \dot{\epsilon} = 2{\cdot}3$. It can be seen that in fact these curves are parallel and have the correct separation over the range 60 to 240 °K, and probably to higher temperatures.

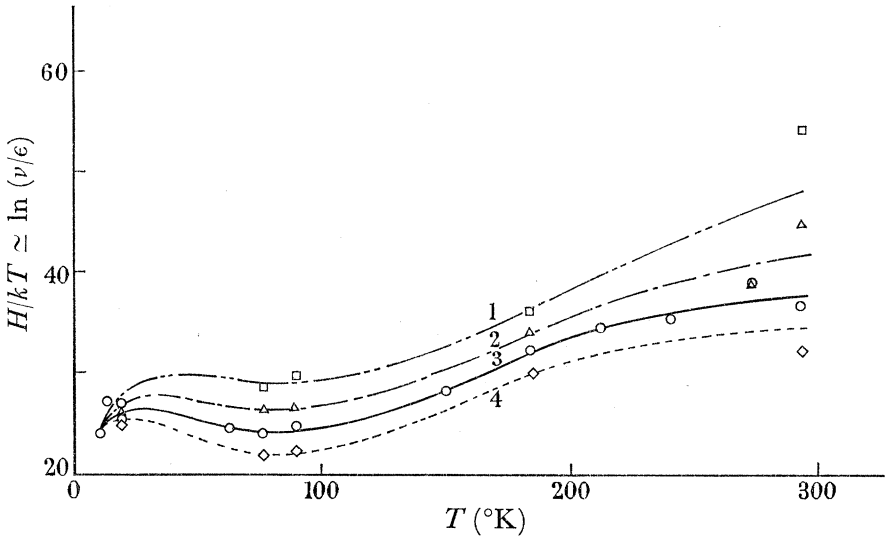

FIGURE 20. Values of $H/kT \approx \ln (v/\dot{\epsilon})$ plotted as a function of temperature for various constant strain rates. Curve 1, $\dot{\epsilon} = 4 \times 10^{-6}$; 2, $\dot{\epsilon} = 4 \times 10^{-5}$; 3, $\dot{\epsilon} = 4 \times 10^{-4}$; 4, $\dot{\epsilon} = 4 \times 10^{-3}$. $\bar{\epsilon} = 0{\cdot}10$.

The results above 240 °K are not accurate because of the small rate of change of flow stress with temperature. The measured differences in H/kT at 20 °K, however, are smaller than expected, and this suggests that either ρ or p may not then be unchanged after a change of temperature or strain rate.

At 293 and 273 °K both the slope of the curve of flow stress against temperature (figure 15) and the value of the strain rate sensitivity (figure 17), decrease with increasing strain, but the former decreases more rapidly so that H/kT also decreases. This is opposite to the result of Conrad & Frederick (1962) and is difficult to understand since it implies a decreasing density of *moving* dislocations. Similar results were obtained by Christian & Masters (1964), who considered possible explanations. However, the slope of the flow stress against temperature curve is so difficult to measure accurately at these temperatures that the effect may result only from experimental error.

Figure 21 shows the ratio of the activation volume to the cube of the Burgers vector plotted as a function of stress for various basic strain rates. A logarithmic plot is used to emphasize the results at high stresses (low temperatures) where v/b^3 is small. The results generally agree well with those previously obtained (see Conrad 1963 for summary) but are

slightly higher than those of Arsenault (1964). The activation volume is roughly independent of strain, except at 20 °K, but is slightly strain rate sensitive.

The low values of the activation volume reinforce the previous argument against impurity interactions as the rate-controlling deformation mechanism. The argument given by Christian & Masters (1964*b*) need not be repeated here; the results show essentially that the product ld is less than $10b^2$ at low temperatures.

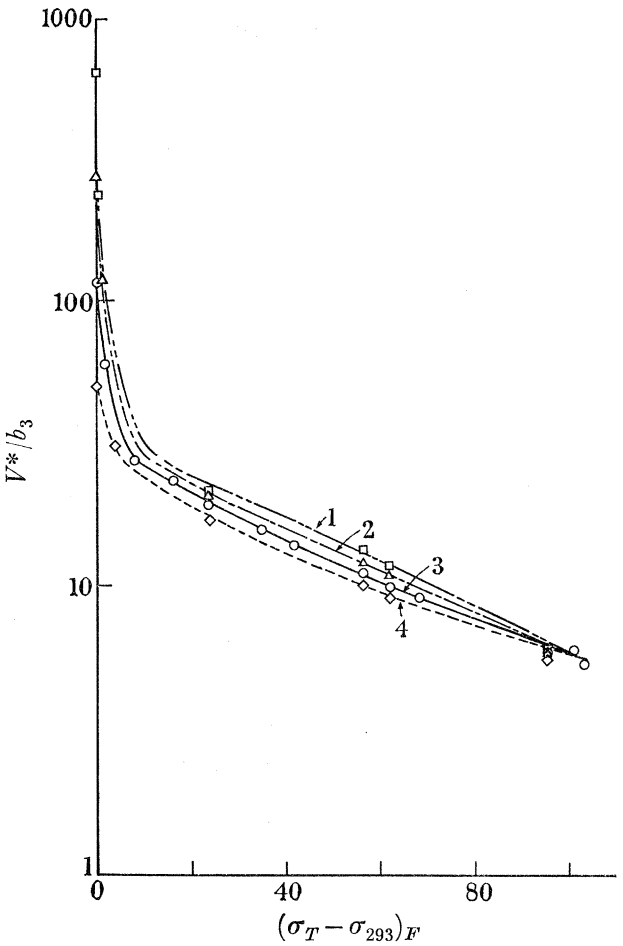

FIGURE 21. The activation volume plotted as a function of stress for various constant strain rates. Curve 1, $\dot{\epsilon} = 4 \times 10^{-6}$; 2, $\dot{\epsilon} = 4 \times 10^{-5}$; 3, $\dot{\epsilon} = 4 \times 10^{-4}$; 4, $\dot{\epsilon} = 4 \times 10^{-3}$. $\bar{\epsilon} = 0{\cdot}10$

To conclude this section, it should be emphasized again that the thermodynamic parameters of the rate equation evaluated above apply to both the polycrystalline material and the very pure single crystals. There is every reason to believe that the rate-controlling mechanism of flow is the same in both materials.

9. STRESS DEPENDENCE OF DISLOCATION VELOCITY

Experiments on the velocities of individual dislocations have usually been interpreted in terms of the empirical relation $u = (\sigma/\sigma_0)^m$ where u is the dislocation velocity and m and σ_0 are material parameters. A similar treatment of the strain rate sensitivity leads to the definition of the parameter $m' = (\partial \ln \dot{\epsilon}/\partial \ln \sigma)_{\epsilon, T}$. In work hardened b.c.c. materials m cannot be measured but m' increases with strain. Provided the density of moving dislocations is not

changed by an incremental change of strain rate, m' and m must be equal but both will vary with strain because of the internal stress field σ_i which develops during work hardening (Christian 1964). It seems logical to expect the velocity of a dislocation to depend only on the effective stress $\sigma^* = \sigma - \sigma_i$ at any one temperature, i.e. $u = (\sigma^*/\sigma_0)^{m^*}$ so that the quantity $m^* = (\partial \ln u/\partial \ln \sigma^*)_{\epsilon, T}$ should not change along the stress against strain curve.

Methods of analysis are now required to check the basic assumption that the density of moving dislocations, ρ, remains constant during an incremental change, and to evaluate m^* and σ^*. Suggestions that the incremental change in density may be calculated from the parameters of the stress against strain curve (Floreen & Scott 1964*a*, *b*) are incorrect as pointed out by Li & Michalak (1964). These authors suggest a test of the basic assumption is to plot the change of stress $\Delta\sigma$ against $(\dot\epsilon_2/\dot\epsilon_1)^{1/m^*}$ where $\dot\epsilon_1$ is fixed and $\dot\epsilon_2$ is a variable. However, this is a very difficult test to apply in practice because of the experimental difficulties in measuring $\Delta\sigma$ for small values of $(\dot\epsilon_2/\dot\epsilon_1)$ and of making rapid changes of strain rate with large values of this ratio.

Suppose that m^* is constant and also that the work hardening is due mainly to σ_i so that σ^* is also approximately constant. Then the change in stress $\Delta\sigma$ between two *fixed* strain rates $\dot\epsilon_1$ and $\dot\epsilon_2$ will also be constant with strain, provided that neither σ_i nor the density of moving dislocations is changed abruptly by the imposed change of strain rate. This is observed experimentally for all the b.c.c. metals. Also since $\Delta\sigma = \Delta\sigma^*$ during the change of strain rate, m^* is given by

$$m^* = \frac{\Delta \ln \dot\epsilon}{\Delta \ln \sigma^*} = \frac{\Delta \ln \dot\epsilon}{\Delta\sigma}\left[\frac{\sigma_1^*}{(1 - \frac{1}{2}(\Delta\sigma/\sigma_1^*) + \frac{1}{3}(\Delta\sigma/\sigma_1^*)^2 - \ldots)}\right]$$

$$= \frac{\Delta \ln \dot\epsilon}{\Delta\sigma}[\sigma_1^* + \tfrac{1}{2}\Delta\sigma - (\Delta\sigma)^2/12\sigma_1^* - \ldots] \qquad (3a)$$

$$= \frac{\Delta \ln \dot\epsilon}{\Delta\sigma}[\sigma_2^* - \tfrac{1}{2}\Delta\sigma - (\Delta\sigma)^2/12\sigma_2^* + \ldots]. \qquad (3b)$$

Thus if $\Delta\sigma \ll \sigma_1^*$, a linear relation should be observed between $\Delta\sigma$ and $\Delta \ln \dot\epsilon$, the slope of which gives σ^*/m^* (or σ/m').

The experimental results for most b.c.c. metals do indicate a linearity between $\Delta\sigma$ and $\ln(\dot\epsilon_2/\dot\epsilon_1)$ for fixed $\dot\epsilon_1$, but the test is not very critical. The result does not, of course, establish the power law, since other relations lead to similar behaviour. For example, if a rate equation is used for dislocation velocity, and the activation volume is assumed to be independent of stress, $\Delta\sigma$ is exactly proportional to $\Delta \ln \dot\epsilon$ when $\Delta\rho = \Delta\sigma_i = 0$. With the power law formulation, it is clear that deviations from linear behaviour will be detected only when σ^* changes fairly rapidly with velocity, that is when m^* is small. Unless such a deviation can be measured, it is not possible to evaluate m^* and σ^* separately.

The rather large variation of strain rate sensitivity with basic rate observed in the present work for iron near room temperature suggests that m^* must be small, and it is then necessary to retain higher terms in the expansion of $\ln(1 + \Delta\sigma/\sigma_1^*)$ in equation (3). Measurement of the stress changes $\Delta\sigma_{12}$ and $\Delta\sigma_{13}$ corresponding to changes from a basic strain rate $\dot\epsilon_1$ to two different strain rates $\dot\epsilon_2$ and $\dot\epsilon_3$, then gives from the first two terms of equation (3*a*)

$$m^*\left[\frac{\Delta\sigma_{13}}{\ln(\dot\epsilon_3/\dot\epsilon_1)} - \frac{\Delta\sigma_{12}}{\ln(\dot\epsilon_2/\dot\epsilon_1)}\right] = \frac{\Delta\sigma_{13} - \Delta\sigma_{12}}{2}. \qquad (4)$$

PHILOSOPHICAL TRANSACTIONS OF THE ROYAL SOCIETY A MATHEMATICAL, PHYSICAL & ENGINEERING SCIENCES

Equation (4) is derived on the assumption that a reproducible value of σ_1^* can be obtained immediately before the two strain rate changes, and strictly this requires two identical specimens to be deformed at strain rate $\dot{\epsilon}_1$ to a defined point on the stress–strain curve. However, there is ample evidence that σ_1^* is determined mainly by temperature and strain rate, and changes only slowly with strain and previous history. Hence values of $\Delta\sigma$ obtained by successive changes of strain rate during the deformation of one specimen may also be used in equation (4) with some confidence. For the same reason, m^* might be determined by using different strain rate ratios and a constant value of upper strain rate $\dot{\epsilon}_2$, by the use of the corresponding equation derived from (3 *b*) by assuming σ_2^* to be constant. This second procedure would be preferable if most of the straining is effected at the higher strain rate.

Table 3 shows values of m^* obtained from equation (4) for strain rate ratios of 50 and 100, and from the corresponding equation when the upper strain rate is constant. There is no systematic variation of the m^* values with strain, but the scatter of the individual $\Delta\sigma$ values is so large that reliable results were not obtained except at room temperature. A rough calculation indicates that with the experimental conditions of this work it would be difficult to measure m^* values exceeding *ca.* 10. The effects of the experimental scatter might be reduced by measuring changes of stress for many different strain rate ratios and using a graphical plot, but this is not possible with the present results.

TABLE 3

temperature (°K)	strain	m^* (equation 4) const. $\dot{\epsilon}_1$	m^* (equation 4) const. $\dot{\epsilon}_2$	m^* (equation 5 and figure 16)
297	0·10	—	—	2·75
—	0·28	3·4	(8)	—
—	0·32	3·9	(6)	—
—	0·36	2·9	(*)	—
273	0·10	—	—	3·35
184	0·10	—	—	40
90	0·10	—	—	27
77	0·10	—	—	26
—	0·20	(8)	28	—
—	0·24	(8)	*	—
20	0·10	—	—	~ 110
14	0·07	*	—	—
—	0·10	—	—	> 140
—	0·15	*	—	—

Bracketed values of m^* from equation (4) are considered unreliable because they require comparison of results from specimens with different mechanical histories. Asterisks, *, indicate that the difference in strain rate sensitivities was too small to be measured, or even (because of experimental scatter) had the wrong sign.

Even with small values of m^*, it is difficult to measure the difference in strain rate sensitivities which appears on the left of equation (4) with sufficient accuracy. It is, however, rather easier to vary $\dot{\epsilon}_1$ over a wide range than it is to vary the ratio $\dot{\epsilon}_2/\dot{\epsilon}_1$, and this suggests the alternative experiment of measuring $\Delta\sigma$ for a fixed strain rate ratio, r, but differing values of $\dot{\epsilon}_1$. Writing $\Delta\sigma = \Delta\sigma_r$ to emphasize these conditions, and rearranging equation (4) of Li & Michalak (1964) gives

$$\begin{aligned}\Delta\sigma_r - \Delta\sigma_i &= \sigma_1^* \left[(\rho_1 r/\rho_2)^{1/m^*} - 1\right] \\ &= \sigma_0 \left[(\rho_1 r/\rho_2)^{1/m^*} - 1\right] (\dot{\epsilon}_1/b\rho_1)^{1/m^*}, \end{aligned} \tag{5}$$

so that if $\rho_1 = \rho_2$ and $\Delta\sigma_i = 0$, a linear relation is predicted between $\ln \Delta\sigma_r$ and $\ln (\dot{\epsilon}_1/\rho_1)$. A possible test of the assumptions is thus to plot $\ln \Delta\sigma_r$ against $\ln \dot{\epsilon}_1$. A linear plot should indicate that ρ_1 (at fixed strain) does not vary appreciably with different strain rates, and the slope of the line gives m^*. This test, in common with that proposed by Li & Michalak, does not really distinguish between $\Delta \ln \rho = 0$ and $\Delta \ln \rho = k \Delta \ln \dot{\epsilon}$ unless m^* is known independently. However, a functional relation between ρ and $\dot{\epsilon}$ seems unlikely.

Figure 16 shows the expected linear relation between $\ln \Delta\sigma_r$ and $\ln \dot{\epsilon}_1$; it is plotted at a fixed strain $\epsilon = 0{\cdot}10$ but the results are essentially valid at all strains. Values of m^* obtained from the slopes of the lines are included in table 3; the results at 184 °K appear to be somewhat anomalous. The values of m^* obtained by the two methods near room temperature agree with each other, and are not substantially different from the value of 5·5 recently obtained by Michalak (1965). Michalak used the method of equation (4) and he also extrapolated m' values to zero strain; the extrapolation technique was not found to be reliable in the present work.

The question of the temperature dependence of m^* is rather difficult. The strain rate results all indicate that m^* becomes much larger at low temperatures, and this would be expected if the velocity were really determined by a rate equation, since this implies that at sufficiently low temperatures $m^* T$ is constant (Christian 1964; Li 1965). However, a recent measurement of m in silicon iron by the etch pit method (Stein & Laforce 1965) indicates a rather small increase in m at low temperatures. Michalak (1965) found a large increase at low temperatures in the values obtained by extrapolating m' to zero strain, but he attributed this to changes in $(\partial \ln \rho / \partial \ln \sigma)_{\dot{\epsilon}, T}$. However, Christian (1964) has previously pointed out that improbably large changes in dislocation density would be required, and he gave other reasons for believing that ρ is constant. In the present work, additional evidence in favour of this assumption (except possibly at 20 °K and below) is given by figures 16 and 20 as already described. It thus seems probable that the increase in m' with decreasing temperature corresponds to a real increase in m^*, as indicated by figure 16 and table 3.

10. Conclusions

The main conclusion from this work is that the large temperature and strain rate sensitivity of the macroscopic flow stress of pure iron cannot be attributed to the residual interstitial impurities. The conclusion is not new, and the theoretical arguments have been fully presented previously (Conrad 1963; Christian & Masters 1964), but the experimental evidence for iron has been rather confused. In the present work, very complete investigations of the temperature and strain rate sensitivity have been made, and in all important respects the results for the very pure single crystals and the moderately pure, zone refined polycrystalline iron were found to be identical.

It is still not possible to decide the dominant mechanism of the friction stress with complete assurance, but the present work strengthens the arguments previously given in favour of a lattice interaction or Peierls–Nabarro force, to use this term in a rather wide sense. Kossowsky & Brown (1966) have also recently concluded that the b.c.c. lattice is responsible for the high macroscopic flow stress of pure iron at low temperatures. Experimental evidence is accumulating that in b.c.c. metals deformed at relatively low temperatures, the dislocations

are straight, parallel to ⟨111⟩ directions, and are fairly uniformly distributed. Experiments with niobium crystals sectioned parallel to the slip plane (Taylor 1965) have confirmed that these dislocations are mainly pure screws, in contrast to the edge dislocation dipoles which are observed in crystals deformed near room temperature.

Another experimental result which is currently attracting much attention is the reported asymmetry of the critical resolved shear stress on the {112} planes with respect to stress direction for silicon–iron (Sestak & Libovicky 1963; Taoka, Takeuchi & Furubayashi 1964) and niobium (Duesbery & Foxall 1965). A possible explanation for this observation is in terms of dislocation decomposition to give stacking faults on intersecting {112} planes, this being one possible cause of a large Peierls–Nabarro force (Hirsch 1960). The iron crystals used in the present work slipped on {110}, but this mechanism could give a large frictional stress for screw dislocations moving on any slip plane.

No attempt has been made in this paper to make detailed comparisons with particular models such as those of Seeger & Schiller (1962) or Dorn & Rajnak (1964). This comparison was made recently by Christian & Masters (1964) and the conclusions reached there are not altered by the present more detailed results. In brief, the models seem to give a correct description of the general features of the temperature and strain rate dependence of the flow stress, and the relevant parameters deduced from the experimental results have reasonable values. Detailed quantitative agreement between the predictions and the actual experimental results is not obtained, presumably because the models are too simple adequately to represent the very complex real conditions of deformation. The Peierls model will not explain the orientation dependence of the yield stress at low temperatures, but this dependence may not exist for the flow stress.

The authors wish to express their gratitude to Dr D. F. Stein for the gift of the single crystals of pure iron, and for helpful discussion and correspondence. They also wish to thank J. W. Halley through whom the zone-refined iron was obtained, and Professor W. Hume-Rothery, F.R.S. for laboratory facilities and accommodation.

References

Adams, M. A. 1959 *J. Sci. Instrum.* **36**, 444.
Allen, N. P., Hopkins, B. E. & McLennan, J. E. 1956 *Proc. Roy Soc.* A, **234**, 221.
Altshuler, T. L. 1964 D.Phil. Thesis, Oxford University.
Altshuler, T. L. & Christian, J. W. 1966 *Acta. Metall.*, **14**, 903.
Arsenault, R. J. 1964 *Acta Metall.* **12**, 547.
Basinski, Z. S. 1959 *Phil. Mag.* **4**, 393.
Basinski, Z. S. & Christian, J. W. 1960 *Austr. J. Phys.* **13**, 299.
Bilby, B. A. Cottrell, A. H. & Swinden, K. H. 1963 *Proc. Roy Soc.* A, **272**, 304.
Boucher, N. A. 1966 Part II Thesis, Oxford University.
Bowen, D. K., Christian, J. W. & Taylor, G. 1967 *Can. J. Phys.* In course of publication.
Brown, N. & Ekvall, R. A. 1962 *Acta Metall.* **10**, 1101.
Campbell, J. D. & Maiden, C. J. 1958 *Phil. Mag.* **3**, 872.
Christian, J. W. 1964 *Acta Metall.* **12**, 99.
Christian, J. W. & Masters, B. C. 1964*a* *Proc. Roy. Soc.* A, **281**, 223.
Christian, J. W. & Masters, B. C. 1964*b* *Proc. Roy. Soc.* A, **281**, 240.
Conrad, H. 1960 *Phil Mag.* **5**, 745.

Conrad, H. 1961 *J. Iron St. Inst.* **198**, 364.
Conrad, H. 1963 *The Relation between structure and mechanical properties of metals*, p. 476. London: H.M.S.O.
Conrad, H. & Frederick, S. 1962 *Acta. Metall.* **10**, 1013.
Conrad, H. & Schoeck, G. 1960 *Acta. Metall.* **8**, 791.
Cottrell, A. H. 1958 *Trans. Am. Inst. Min.* (*Metall.*) *Engrs* **212**, 192.
Cottrell, A. H. 1963 *The relation between structure and mechanical properties of metals*, p. 456. London: H.M.S.O.
Davidenkov, N. N. & Chuman, T. N. 1960 *Physics of Metals Metallogr.* **9**, 741.
Dingley, D. J. 1963 *The relation between structure and mechanical properties of metals*, p. 690. London: H.M.S.O.
Dorn, J. E. & Rajnak, S. 1964 *Trans. Am. Inst. Min.* (*Metall.*) *Engrs.* **230**, 1052.
Duesbury, M. S. & Foxall, R. A. 1965 *Symposium Reinststoffe in Wissenschaft und Tecknik. Dresden.*
Edmondson, B. 1961 *Proc. Roy. Soc.* A, **164**, 176.
Erickson, J. S. & Low, J. R. 1957 *Acta Metall.* **5**, 405.
Erickson, J. S. & Low, J. R. 1959 *Acta Metall.* **7**, 58.
Floreen, S. & Scott, T. E. 1964*a* *Acta Metall.* **12**, 758.
Floreen, S. & Scott, T. E. 1964*b* *Acta Metall.* **12**, 1459.
Glen, J. W. 1956 *Phil. Mag.* **1**, 400.
Gorsuch, P. D. 1959 *G.E. Lab. Progr. Rep.* October 1959.
Guiu, F. & Pratt, P. L. 1966 *Phys. Stat. Sol.* **15**, 539.
Hamer, F. M. & Hull, D. 1964 *Acta. Metall.* **12**, 682.
Heslop, J. & Petch, N. J. 1956 *Phil Mag.* **1**, 866.
Hirsch, P. B. 1960 *Fifth Int. Congr. Crystallography*, Cambridge.
Johnson, A. A. 1962 *Acta Metall.* **10**, 975.
Johnston, W. G. 1962 *J. Appl. Phys.* **33**, 2050.
Keh, A. S. 1965 *Phil. Mag.* **12**, 9.
Kossowsky, R. & Brown, N. 1966 *Acta Metall.* **14**, 131.
Lawley, A., Van den Sype, J. & Maddin, R. 1962–3 *J. Inst. Met.* **91**, 23.
Lean, J. B. 1960 *Aust. J. Phys.* **13**, 359.
Li, J. C. M. 1965 *Trans. Amer. Inst. Min.* (*Metall.*) *Engrs* **233**, 219.
Li, J. C. M. & Michalak, J. T. 1964 *Acta Metall.* **12**, 1457.
Lindley, T. C. & Smallman, R. E. 1963 *Acta Metall.* **11**, 361.
Louat, N. 1956 *Proc. Phys. Soc.* B**69**, 454.
Louat, N. 1959 *Acta Metall.* **7**, 57.
Low, J. R. 1963 *Iron and its dilute solid solutions*, p. 217. New York: Interscience Publishers.
Marsh, K. J. & Campbell, J. D. 1963 *J. Mech. Phys. Solids* **11**, 49.
Michalak, J. T. 1965 *Acta Metall.* **13**, 213.
Mitchell, T. E. Foxall, R. A. & Hirsch, P. B. 1963 *Phil Mag.* **8**, 1895.
Mitchell, T. E. & Spitzig, W. A. 1965 *Acta Metall.* **13**, 1169.
Mogford, I. L. & Hull, D. 1963 *J. Iron St. Inst.* **201**, 55.
Mordike, B. L. & Haasen, P. 1962 *Phil. Mag.* **7**, 459.
Mott, N. F. 1956 *Phil. Mag.* **1**, 567.
Petch, N. J. 1964 *Acta Metall.* **12**, 59.
Phillips, R. & Chapman, J. A. 1965 *J. Iron St. Inst.* **203**, 511.
Read, T. A., Markus, H. & McCaughey, J. M. 1952 *Fracturing of metals*, p. 228. Cleveland, Ohio, American Society for Metals.
Rose, R. M., Ferriss, D. P. & Wulff, J. 1962 *Trans. Amer. Inst. Min.* (*Metall.*) *Engrs.* **224**, 981.
Rosenfield, A. R. 1962–3 *J. Inst. Metals* **91**, 104.
Samuels, L. E. 1956–7 *J. Inst. Metals* **85**, 51.
Samuels, L. E. 1957–8 *J. Inst. Metals* **86**, 43.

PHILOSOPHICAL TRANSACTIONS OF THE ROYAL SOCIETY A MATHEMATICAL, PHYSICAL & ENGINEERING SCIENCES

Seeger, A. & Schiller, P. 1962 *Acta Metall.* **10**, 348.
Sestak, B. & Libovicky, S. 1963 *The relation between structure and mechanical properties of metals*, p. 158. London: H.M.S.O.
Schoeck, G. 1965 *Phys. Stat. Sol.* **8**, 499.
Sleeswyk, A. W. & Helle, J. N. 1963 *Acta Metall.* **11**, 187.
Stein, D. F. 1963 Ph.D. Thesis, Rensselar Polytechnic Institute, Troy N.Y.
Stein, D. F. 1966 *Acta Metall.* **14**, 99.
Stein, D. F. 1967 *Canad. J. Phys.* In course of publication.
Stein, D. F. & Laforce, R. P. 1965 *J. Appl. Phys.* **36**, 661.
Stein, D. F. & Low, J. R. 1966 *Acta Metall.* **14**, 1183.
Stein, D. F., Low, J. R. & Seybolt, A. U. 1963 *Acta Metall.* **11**, 1253.
Taoka, T., Takeuchi, S. & Furubayashi, E. 1964 *J. Phys. Soc. Japan* **19**, 702.
Taylor, G. 1965 D.Phil. Thesis, Oxford University.
Taylor, G. & Christian, J. W. 1965 *Acta Metall.* **13**, 1216.
White, G. K. 1962 *Cryogenics* **2**, 292.

Appendix I. Errors due to imperfect specimen preparation

Figure A1 shows a vertical section through an imperfectly prepared compression specimen in which the normal to the end faces makes a small angle, α, with the specimen axis, and the distance of the centre of a face from a vertical line MM through the centre of pressure is δ. The separation of the ends of the specimen measured normal to the compression anvils is h, and the end faces are assumed to be either circular with radius r, or rectangular with one side of length $2X$ in the plane of figure A1.

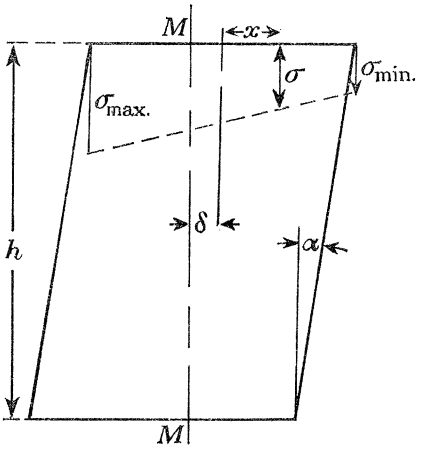

Figure A1. Section through compression specimen with axis not perpendicular to end faces.

Since the end faces remain flat, it is readily seen that the stress during elastic loading varies linearly with the x co-ordinate from $\sigma_{\text{max.}}$ to $\sigma_{\text{min.}}$ where

$$\sigma_{\text{max.}} + \sigma_{\text{min.}} = 2\sigma_{\text{av.}}$$

and $\sigma_{\text{av.}}$ is equal to the applied load divided by the area of the face.

The condition for static equilibrium is that the moment about M shall vanish, and this gives

$$\sigma_{\text{max.}} = \sigma_{\text{av.}}(1 + 3\delta/X)$$

or

$$\sigma_{\text{max.}} = \sigma_{\text{av.}}(1 + 4\delta/r)$$

for rectangular and circular specimens respectively. Since $2\delta = h\tan\alpha \approx h\alpha$, and for most of the specimens used in the present work $h/X = 4$ or $h/r = 4$, these equations reduce to

$$\sigma_{\max.} = \sigma_{\text{av.}}(1+6\alpha)$$

for rectangular specimens and $\sigma_{\max.} = \sigma_{\text{av.}}(1+8\alpha)$

for circular specimens.

One polycrystalline iron specimen was deliberately prepared with $\alpha \sim 1^\circ \sim 0{\cdot}017$ rad. In all other respects, this specimen was identical with the Fe PX 2 series, and was annealed with them. When tested at 20·4 °K at a plastic strain rate of $4\times10^{-4}\,\text{s}^{-1}$, the extrapolated yield stress was found to be $\sigma_{\text{av.}} = 70{\cdot}2\,\text{Kg/mm}^2$, which is significantly smaller than the values obtained from the remaining PX 2 specimens. The calculated value of $\sigma_{\max.}$ using the above equation is 79·7 Kg/mm^2, and this agrees well with the yield stress of $81{\cdot}7 \pm 3{\cdot}5$ Kg/mm^2 which represent the 95 % probability limits of all other determinations.

This experiment shows that imperfectly prepared specimens begin to yield when $\sigma_{\max.}$ rather than $\sigma_{\text{av.}}$ reaches the macroscopic yield stress, and it emphasizes the necessity for very careful specimen preparation in compression testing. As is shown by the above figures, a value of α of only 1° gives a 13 % error in the measured yield stress. This is believed to be the reason for the larger scatter in the results obtained with the preliminary (PX1) specimens.

Appendix II. Changes of stress in barrelled specimens

Figure A 2 shows a change of temperature or strain rate producing a change in measured stress $\Delta\sigma_m$. Let the stress of a uniformly deformed specimen at strain ϵ be σ_0, and let δ be the error due to barrelling, so that $\sigma_0 = (1-\delta)\,\sigma_m$ and $\Delta\sigma_0 = (1-\delta)\,\Delta\sigma_m + \sigma_m\Delta\delta$. Since the strain, $\Delta\epsilon$, between a and b is elastic, there should be virtually no change in δ; however, in principle a small change may be involved, as shown schematically in figure A 3. This change can be considered linear with strain, so that $\Delta\delta/\Delta\epsilon = \beta(\delta/\epsilon)$ where β is a proportionality constant chosen at point (a). Also $\Delta\sigma_m/\Delta\epsilon = E = \lambda(\sigma_m/\epsilon)$, where E is the elastic modulus and λ is therefore a large number These equations give $\Delta\sigma_0 = [1-\delta-(\beta/\lambda)\,\delta]\,\Delta\sigma_m$ where necessarily $\beta < 1$ and $\lambda > 10$ for $\epsilon > 0{\cdot}05$. This means $\beta/\lambda < 0{\cdot}1$ and can be neglected so that

$$\frac{\Delta\sigma_0}{\sigma_0} = \frac{\Delta\sigma_m}{\sigma_m}.$$

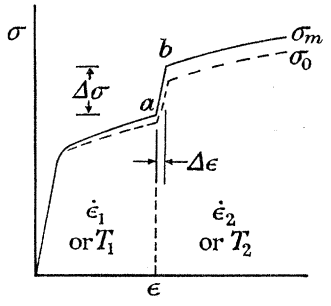

Figure A 2

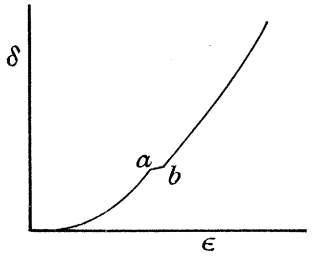

Figure A 3

Figure A 2. To illustrate the effect of a change of strain rate or temperature on the true stress (σ_0) and the measured stress (σ_m) in a slightly barrelled specimen.

Figure A 3. The parameter $\delta = 1-\sigma_0/\sigma_m$ as a function of strain during the incremental change shown in figure A 2.